

Discovery and Development of Thiazolo[3,2-*a*]pyrimidinone Derivatives as General Inhibitors of Bcl-2 Family Proteins

Bingcheng Zhou,^[a] Xun Li,^[a] Yan Li,^[a] Yaochun Xu,^[a] Zhengxi Zhang,^[a] Mi Zhou,^[a] Xinglong Zhang,^[a] Zhen Liu,^[a] Jiahai Zhou,^[a] Chunyang Cao,^[a] Biao Yu,^{*,[a]} and Renxiao Wang^{*,[a, b]}

A class of compounds with a common thiazolo[3,2-*a*]pyrimidinone motif has been developed as general inhibitors of Bcl-2 family proteins. The lead compound was originally identified in a random screening of a small compound library using a fluorescence polarization-based competitive binding assay. Its binding to the Bcl-x_L protein was further confirmed by ¹⁵N-HSQC NMR experiments. Structural modifications on the lead

compound were guided by the outcomes of molecular modeling studies. Among the 42 compounds obtained, a number of them exhibited much improved binding affinities to Bcl-2 family proteins as compared to the lead compound. The most potent compound, BCL-LZH-40, inhibited the binding of BH3 peptides to Bcl-x_L, Bcl-2, and Mcl-1 with inhibition constants (*K*_i) of 17, 534, and 200 nM, respectively.

Introduction

As key regulators of cell apoptosis, Bcl-2 family proteins (including Bcl-2, Bcl-x_L, Mcl-1 etc.) have drawn much attention since the late 1990s.^[1–6] Various types of tumor cells overexpress at least one of these proteins, which protect these tumor cells from apoptosis. Recent studies revealed that Bcl-2 family proteins also play important roles in other cellular events, such as autophagy^[7] and cell proliferation.^[8] Thus, development of small-molecule inhibitors targeting Bcl-2 family proteins is a promising approach for the development of new anticancer therapies.^[9–11] A range of small-molecule inhibitors of Bcl-2 family proteins have been reported in recent years, such as ABT-737 and ABT-263,^[12,13] BH3I compounds,^[14] gossypol and its derivatives,^[15,16] GX15-070,^[17] TW-37,^[18] TM-179,^[19] BI-97C1,^[20] and Incednine.^[21] Some of them, for example, ABT-263, gossypol (AT-101), and GX15-070, have already entered clinical trials.^[10]

Bcl-2 family proteins carry out their biological functions through interactions with other proteins. It is relatively difficult to develop effective small-molecule regulators of protein–protein interactions. Despite all of the successful efforts mentioned above, the structural diversity of known Bcl-2 inhibitors is still very limited as compared to some other established drug targets. It is therefore worthwhile to continue the development of new classes of compounds as effective inhibitors of Bcl-2 family proteins so that more drug candidates can be eventually identified for clinical trials.

We have discovered and developed a class of compounds, all of which have a thiazolo[3,2-*a*]pyrimidinone motif, as general inhibitors of Bcl-2 family proteins. Their binding to the Bcl-2 family proteins was confirmed by an in vitro binding assay as well as HSQC NMR measurements. Our best compound achieved tight binding to Bcl-x_L with *K*_i = 17 nM, which is compara-

ble to ABT-737, a well-known potent small-molecule inhibitor of Bcl-2 family proteins. This class of compounds has certain advantages and may serve as a good starting point for developing even more potent inhibitors of Bcl-2 family proteins.

Results and Discussion

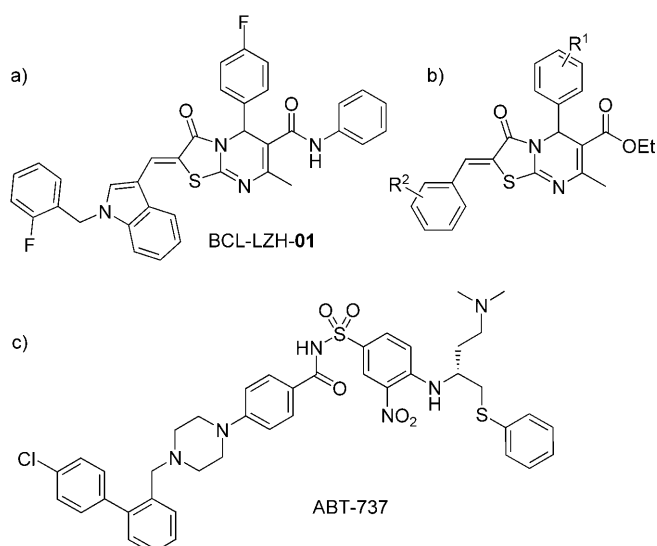
Lead discovery

A fluorescence polarization (FP)-based competitive binding assay was used to screen plausible inhibitors of Bcl-x_L, Bcl-2, and Mcl-1 proteins. An in-house collection of 95 compounds, which was originally purchased from the SPECS company (<http://www.specs.net/>), was screened for testing in this in vitro binding assay. Encouragingly, one compound, BCL-LZH-01 (Scheme 1), exhibited modest inhibitory activities against all three target proteins, with *K*_i values of 1.64, 2.67, and 1.05 μM against Bcl-x_L, Bcl-2, and Mcl-1, respectively. As BCL-LZH-01 was obtained from a commercial inventory, we searched published literature to examine whether any similar compounds

[a] B. Zhou, Dr. X. Li, Dr. Y. Li, Y. Xu, Z. Zhang, M. Zhou, Dr. X. Zhang, Dr. Z. Liu, Prof. J. Zhou, Prof. C. Cao, Prof. B. Yu, Prof. R. Wang
State Key Laboratory of Bioorganic Chemistry
Shanghai Institute of Organic Chemistry, Chinese Academy of Sciences
345 Lingling Road, Shanghai 200032 (P. R. China)
Fax: (+86) 21-64166128
E-mail: wangrx@mail.sioc.ac.cn
byu@mail.sioc.ac.cn

[b] Prof. R. Wang
State Key Laboratory of Natural and Biomimetic Drugs
Peking University, Beijing 100191 (P. R. China)

Supporting information for this article is available on the WWW under <http://dx.doi.org/10.1002/cmdc.201000484>.



Scheme 1. a) The lead compound (SPECS ID: AH-487/40936177) identified in our study. b) Compounds reported by Braud et al. as CDC25B phosphatase inhibitors.^[22] c) ABT-737, a well-known potent inhibitor of Bcl-2 family proteins developed by Abbott Labs,^[12,13] which was used as a positive control in our study.

had been studied before. We found that Braud et al. reported a class of compounds with essentially the same framework (Scheme 1) as CDC25B phosphatase inhibitors with an optimal IC_{50} value of 4.5 μM .^[22] However, it seems that binding to Bcl-2 family proteins is still a new application of this class of compounds. Also, the chemical structure of BCL-LZH-01 is notably different from Braud's compounds. We thus decided to explore the potential of this class of compound as effective Bcl-2 family protein inhibitors by choosing BCL-LZH-01 as the lead compound.

The template compound

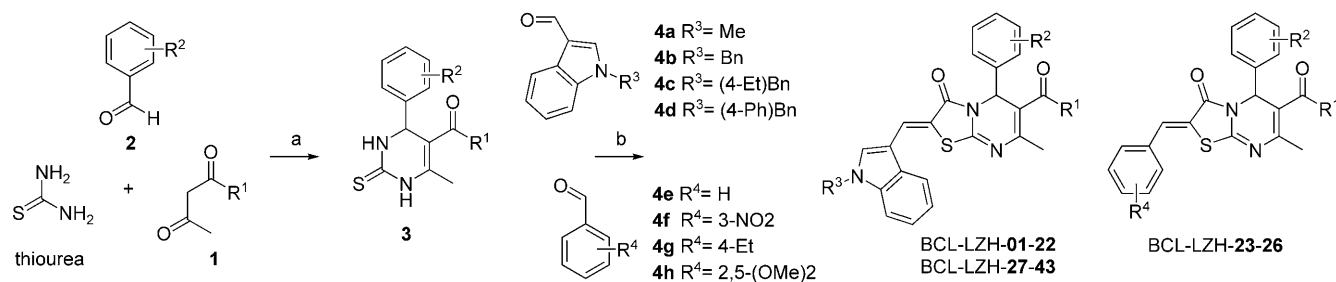
The chemical structure of BCL-LZH-01 is fairly complicated as a lead compound. We thus designed a simplified molecular structure by removing the two fluorine substituent groups on BCL-LZH-01 and used it as a template for further modifications. The resulting compound, that is, BCL-LZH-02, was synthesized using the methods shown in Scheme 2. Encouragingly, this compound already achieved considerably better binding affini-

ties than BCL-LZH-01 with K_i values of 0.11 μM and 0.37 μM against Bcl-x_L and Bcl-2, respectively (Table 1).

As an additional method for confirming the binding of BCL-LZH-02, heteronuclear single quantum coherence (HSQC) NMR spectroscopy was performed using uniformly ^{15}N -labeled Bcl-x_L protein. Conformational changes of a protein molecule induced by the binding of a small-molecule ligand will result in peak shifts on a ^{15}N -HSQC spectrum, providing direct evidence for the binding of the ligand molecule. In our study, a ^{15}N -HSQC NMR spectrum of Bcl-x_L was recorded with and without the presence of BCL-LZH-02. Comparison of the two resulting HSQC spectra revealed a number of induced shifts (Figure 1 a), indicating that BCL-LZH-02 does interact with some residues on Bcl-x_L. ABT-737 (Scheme 1) was also tested in our HSQC NMR measurements. ABT-737 inhibited the binding of the Bim-BH3 peptide to Bcl-x_L with a K_i value of 18 nM in our binding assay. Comparing the HSQC spectra of Bcl-x_L with either BCL-LZH-02 or ABT-737, shows that the residues on Bcl-x_L affected by the binding of BCL-LZH-02 overlap nicely with those affected by the binding of ABT-737 (Figure 1 b). This observation clearly demonstrated that BCL-LZH-02 and ABT-737 bind to the same site on Bcl-x_L.

Molecular modeling

To provide a rational guide for subsequent structural modifications, molecular modeling was employed to predict the binding mode of BCL-LZH-02 with Bcl-x_L. The three-dimensional structure of Bcl-x_L considered in our modeling was taken from Protein Data Bank (PDB entry 1BXL), a NMR-resolved structure of Bcl-x_L in complex with the Bak-BH3 peptide.^[23] Firstly, some binding models were generated by molecular docking using the GOLD software. It should be mentioned that there is a chiral center on the dihydropyrimidine ring in the chemical structure of BCL-LZH-02 (Scheme 2). Therefore, we considered both the *R* and the *S* enantiomer in our study and derived both their binding modes. Each binding mode was further evaluated by molecular dynamics (MD) simulations 3 ns long in explicit water by using the AMBER software. Our MD results indicated that the overall binding modes of the *R* and *S* enantiomer of BCL-LZH-02 are similar. They can be placed inside the binding site on Bcl-x_L in a similar way because the thiazolo[3,2-a]pyrimidinone moiety in their structures can take two different orientations. Based on the binding modes of the *R* and



Scheme 2. Synthesis of thiazolo[3,2-a]pyrimidinone derivatives BCL-LZH-02–43. Reagents and conditions: a) *p*-TsOH-H₂O, EtOH, reflux, 24 h, 21–100%; b) 2-chloroacetic acid, HOAc, Ac₂O, NaOAc, 80 °C, 24 h, 3–68%.

Table 1. Binding affinities of the BCL-LZH compounds to three Bcl-2 family proteins measured using a FP-based in vitro binding assay.

Compd	R ¹	R ²	R ³	R ⁴	Bcl-x _L	K _i [μM] ^[a] Bcl-2	Mcl-1
BCL-LZH-01	NHPh	4-F	(2-F)-Bn	–	1.64	2.67	1.05
BCL-LZH-02	NHPh	H	Bn	–	0.11	0.37	> 100 ^b
BCL-LZH-03	NHPh	4-Br	Bn	–	0.50	0.86	0.99
BCL-LZH-04	NHPh	4-OMe	Bn	–	0.25	> 100	> 100
BCL-LZH-05	NHPh	4-Et	Bn	–	0.081	1.36	> 100
BCL-LZH-06	NHPh	3-OAc	Bn	–	0.12	0.16	1.96
BCL-LZH-07	NHPh	4-OAc	Bn	–	0.12	0.31	> 100
BCL-LZH-08	NHPh	3,4-(OAc) ₂	Bn	–	0.21	0.27	1.47
BCL-LZH-09	OEt	H	Bn	–	0.79	1.37	1.55
BCL-LZH-10	OEt	3-Cl	Bn	–	0.27	1.28	1.06
BCL-LZH-11	OEt	3-OMe	Bn	–	0.12	0.37	1.16
BCL-LZH-12	OEt	4-Et	Bn	–	0.11	2.42	1.83
BCL-LZH-13	N(Me)Ph	H	Bn	–	> 100	> 100	> 100
BCL-LZH-14	NHMe	H	Bn	–	0.96	2.92	> 100
BCL-LZH-15	OMe	H	Bn	–	0.21	1.88	5.64
BCL-LZH-16	N(Me)Ph	4-OAc	Bn	–	> 100	> 100	> 100
BCL-LZH-17	NHMe	4-OAc	Bn	–	0.98	11.33	> 100
BCL-LZH-18	OMe	4-OAc	Bn	–	0.11	0.45	0.58
BCL-LZH-19	NHPh	H	Me	–	0.15	1.48	0.54
BCL-LZH-20	NHPh	3-OAc	Me	–	0.43	0.86	0.63
BCL-LZH-21	NHPh	4-OAc	Me	–	0.26	1.92	2.44
BCL-LZH-22	NHPh	3,4-(OAc) ₂	Me	–	2.03	0.94	1.65
BCL-LZH-23	NHPh	H	–	H	> 100	> 100	> 100
BCL-LZH-24	NHPh	3,4-(OAc) ₂	–	3-NO ₂	> 100	> 100	> 100
BCL-LZH-25	OEt	H	–	4-Et	> 100	> 100	> 100
BCL-LZH-26	OEt	4-Et	–	2,5-(OMe) ₂	2.76	> 100	> 100
BCL-LZH-27	NHPh	H	4-Et-Bn	–	0.54	0.98	> 100
BCL-LZH-28	NHPh	4-OAc	4-Et-Bn	–	0.14	0.33	0.99
BCL-LZH-29	NHPh	3,4-(OAc) ₂	4-Et-Bn	–	0.24	0.92	1.22
BCL-LZH-30	OEt	H	4-Et-Bn	–	0.18	1.66	1.05
BCL-LZH-31	OMe	4-OAc	4-Et-Bn	–	0.095	1.16	0.37
BCL-LZH-32	NHPh	H	4-Ph-Bn	–	0.078	1.07	> 100
BCL-LZH-33	NHPh	4-F	4-Ph-Bn	–	0.11	3.06	> 100
BCL-LZH-34	NHPh	3-Cl	4-Ph-Bn	–	0.086	0.97	1.49
BCL-LZH-35	NHPh	4-Br	4-Ph-Bn	–	0.061	2.75	8.54
BCL-LZH-36	NHPh	4-Et	4-Ph-Bn	–	0.29	0.88	5.51
BCL-LZH-37	NHPh	3-OAc	4-Ph-Bn	–	0.13	0.15	0.90
BCL-LZH-38	NHPh	4-OAc	4-Ph-Bn	–	0.16	0.45	> 100
BCL-LZH-39	NHPh	3,4-(OAc) ₂	4-Ph-Bn	–	0.035	1.15	0.45
BCL-LZH-40	OEt	H	4-Ph-Bn	–	0.017	0.53	0.20
BCL-LZH-41	OEt	4-F	4-Ph-Bn	–	0.089	0.57	0.80
BCL-LZH-42	OEt	3-OMe	4-Ph-Bn	–	0.067	1.04	0.44
BCL-LZH-43	OMe	4-OAc	4-Ph-Bn	–	0.14	0.73	1.52
ABT-737	–	–	–	–	0.018	0.074	> 100

[a] The K_i value is the average of two independent experiments. Each experiment included three parallel measurements at every concentration. [b] No obvious inhibitory activity was observed up to 10 μM. We therefore estimated that the K_i values in these cases should be well above 100 μM.

S enantiomers derived from our MD simulations, the binding energies computed by the MM-GB/SA method implemented in AMBER favored the *R* enantiomer, that is, $-14.7 \text{ kcal mol}^{-1}$ versus $-9.3 \text{ kcal mol}^{-1}$ (refer to the Supporting Information for more details).

The predicted binding mode of the *R* enantiomer of BCL-LZH-02 is shown in Figure 2a. This predicted binding mode suggests that 1) the indole moiety together with the *N*-benzyl group have close contacts with the hydrophobic residues around subpocket A, 2) the phenyl group linked to the chiral

center on the dihydropyrimidine ring resides in subpocket B, another hydrophobic environment. The thiazolo[3,2-*a*]pyrimidinone moiety on BCL-LZH-02 acts as a linker between two subpockets. The several heteroatoms on it do not form hydrogen bonds with any nearby residues. This predicted binding mode has an obvious overall similarity with the experimentally resolved binding mode of ABT-737 (Figure 2b), although the chemical structures of these two molecules are quite different (Scheme 1). This similarity is also consistent with our HSQC results.

Chemistry

A total of 42 derivative compounds of the template compound were synthesized (Table 1). These compounds were designed to explore the influence of different substitutions on the core structure. The synthetic methods for BCL-LZH-02–43 are given in Scheme 2. In brief, dihydropyrimidine derivatives **3a–3t** were prepared by the classic Biginelli reaction^[24,25] of commercially available β -keto ester or amide **1**, differentially substituted aldehyde **2**, and thiourea in reflux ethanol, which was catalyzed by *p*-toluenesulfonic acid monohydrate. The overall yields of this step were between 21% and 100%. Biginelli products **3a–3t** were then reacted with varied aldehydes **4a–4h** and 2-chloroacetic acid in the presence of acetic acid,

acetic anhydride, and sodium acetate at 80°C to obtain BCL-LZH-02–43.^[26] Differentially substituted aldehydes **4e–4h** were purchased from commercial sources. *N*-substituted 1*H*-indole-3-carbaldehyde **4a–4d** were prepared from 1*H*-indole-3-carbaldehyde **8** with iodomethane **7a** or various substituted benzyl bromides. Those substituted benzyl bromides were either commercial available (**7b**) or could be prepared (**7c**, **7d**) from substituted benzyl alcohols in overall yields of 68% to 87% (Scheme 3).

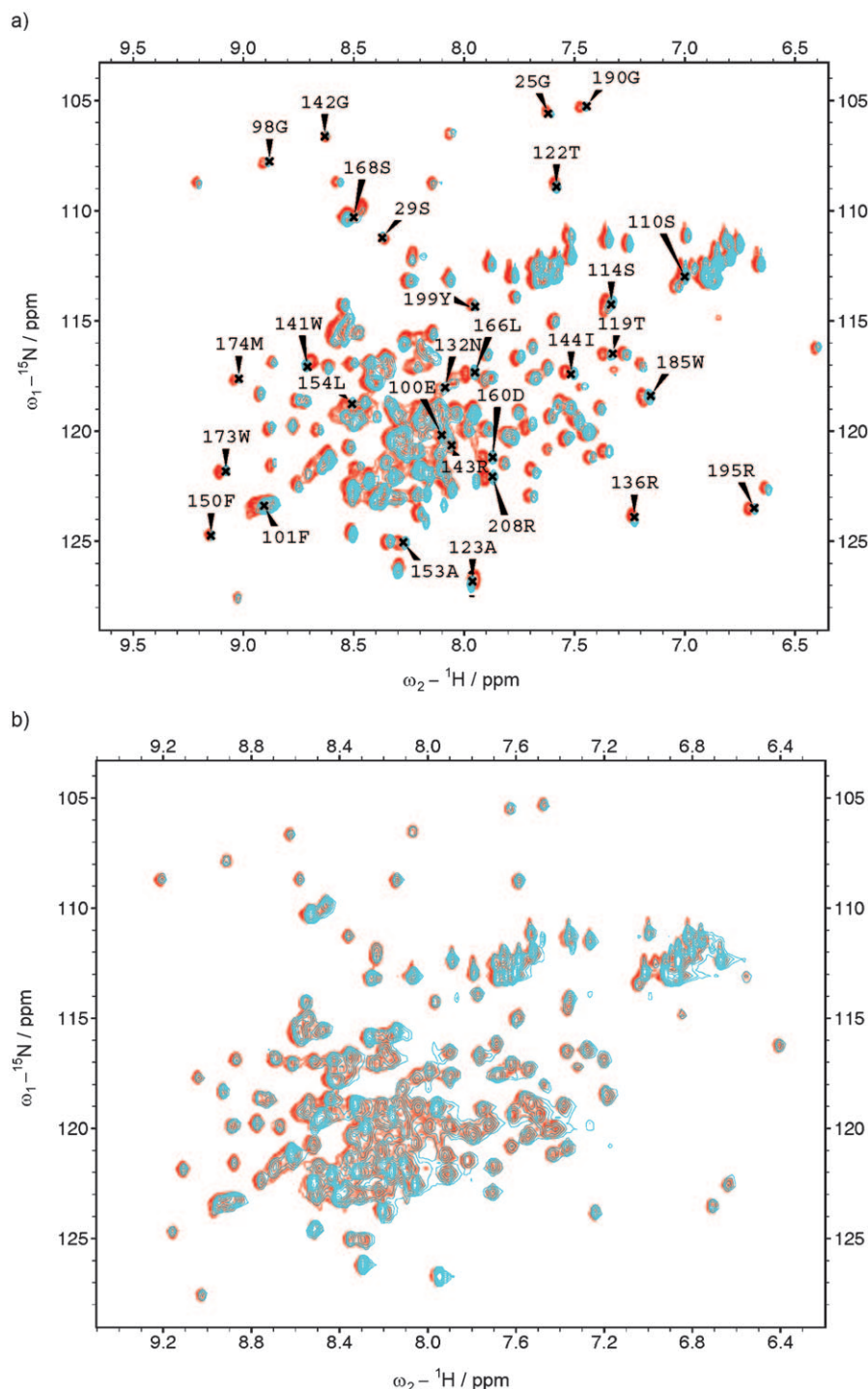


Figure 1. a) Superposition of the two ^{15}N -HSQC spectra of Bcl- x_L in free form (cyan) and in the presence of BCL-LZH-02 (red). Peaks with induced shifts in the presence of BCL-LZH-02 are labelled with the corresponding residue numbers. b) Superposition of the two ^{15}N -HSQC spectra of Bcl- x_L at the presence of ABT-737 (cyan) and BCL-LZH-02 (red).

Analysis of the structure–activity relationships

Inhibitory activities of the new BCL-LZH compounds against three Bcl-2 family proteins are summarized in Table 1. To derive the structure–activity relationship of this class of compounds, we predicted the binding modes of the active compounds to Bcl- x_L through molecular docking. Bcl- x_L was chosen

as this class of compounds was generally more potent on Bcl- x_L than Bcl-2 or Mcl-1 and thereby the corresponding structure–activity relationship may be more straightforward to interpret.

We explored three main sites on the framework of this class of compounds for possible modifications in our study (Scheme 2). For the convenience of organic synthesis, we first tested different substituent groups as R^1 and R^2 by using various reactants in the Biginelli reaction. The predicted binding mode of the template compound (Figure 2a) suggested that the phenylamide group as R^1 may form π - π interactions with a nearby Tyr195 residue. Also, as R^1 is essentially exposed to the solvent, we also considered the use of either a methyl or an ethyl ester group as R^1 . As for the substituted phenyl moiety R^2 , the predicted binding mode of the template compound (Figure 2a) suggested that this moiety is located in the hydrophobic subpocket B. Thus, R^2 should be a small, simple group. In our study, we tested some small alkyl groups, halogen groups, a methoxy group, and an acetoxyl group as R^2 .

These design ideas led to compounds BCL-LZH-03–18 (Table 1). One can see that if the phenylamide group was replaced by a methyl or an ethyl ester group, activities of the resulting compounds (BCL-LZH-09–12, BCL-LZH-15, and BCL-LZH-18) were generally comparable to those compounds with a phenylamide group as R^1 (BCL-LZH-02–08). This is consistent with our prediction that R^1 is largely exposed to the solvent so that a hydrophilic group at this site is a reasonable choice. Interestingly, if the nitrogen atom on the phenylamide group is methylated, the resulting compounds (BCL-LZH-13 and BCL-LZH-16) essentially lost activities on all three target proteins. When the phenylamide group was replaced by a methylamide group, activities of the resulting compounds (BCL-LZH-14 and BCL-LZH-17) were also

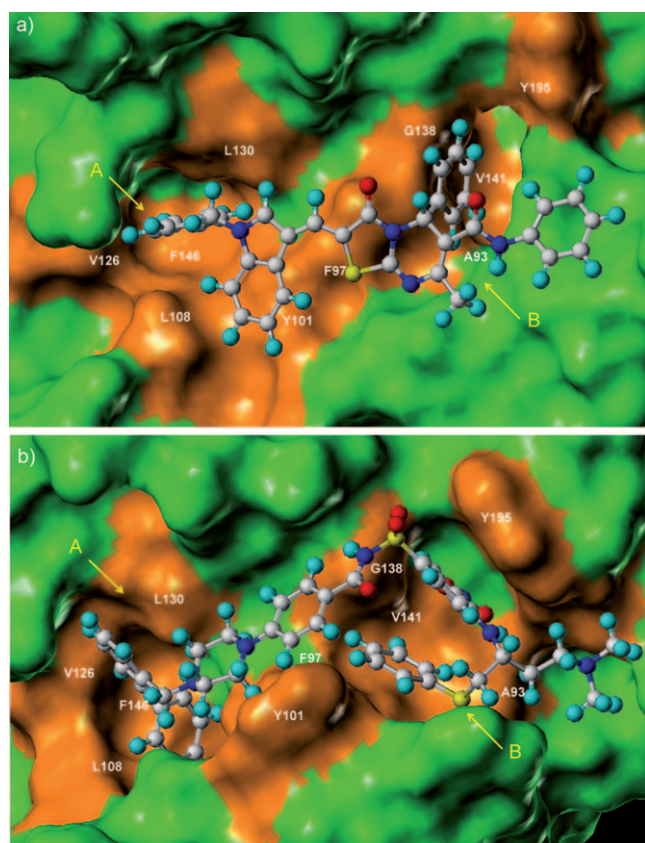
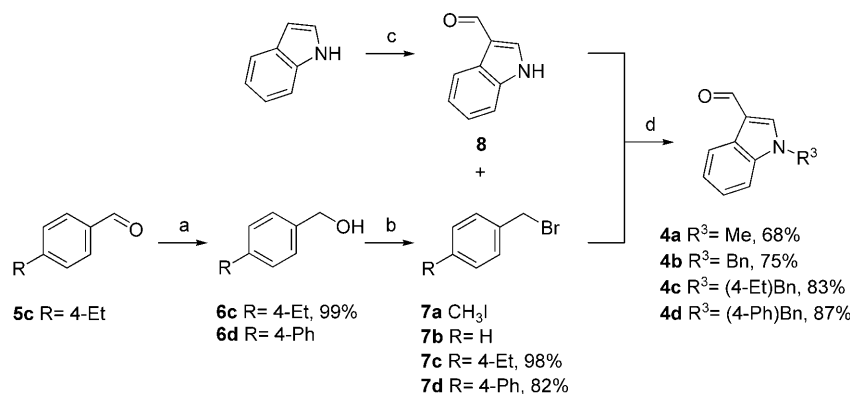


Figure 2. a) Predicted binding mode of BCL-LZH-02 with Bcl- x_L . b) The experimentally resolved structure of Bcl- x_L in complex with ABT-737 (PDB entry 2YXJ). Subpocket A is formed mainly by Phe97, Tyr101, Leu108, Val126, Leu130, and Phe146; subpocket B is formed mainly by Ala93, Gly138, Val141, and Tyr195. These hydrophobic residues are colored in orange on the molecular surface of Bcl- x_L ; whereas other residues are colored in green.



Scheme 3. Synthesis of *N*-substituted indole-3-aldehyde **4a–4d**. Reagents and conditions: a) NaBH_4 , CH_3OH , 0°C , 30 min; b) PBr_3 , CH_2Cl_2 , 0°C , 6 h; c) POCl_3 , DMF, 0°C , 1 h, then RT, 3 h, 95%; d) NaH , THF, 0°C , 10 min, then RT, 1 h.

clearly worse than the template compound (BCL-LZH-02). These observations reveal the subtle role of the phenylamide group, implying that this group may form specific interactions with nearby residues such as Tyr195.

As for R^2 , different types of substituent groups actually did not make much difference in the activities of the resulting compounds. As mentioned earlier, the substituted phenyl

moiety R^2 was predicted to locate in the hydrophobic subpocket B (Figure 2a). Hydrophobic effects should be dependent primarily on the sizes of chemical groups rather than their types. Thus, this observation is not totally unexpected. Here, it seems that a substituent group at the para-position on the phenyl ring, such as BCL-LZH-05, BCL-LZH-12, and BCL-LZH-18, is favorable for achieving better activities.

We then turned our attention to the role of R^3 . First, we synthesized a few compounds by replacing the *N*-benzyl group on the indole moiety with a simple *N*-methyl group (BCL-LZH-19 to -22). Such modifications were not helpful in terms of improving activities. Our molecular docking results indicated that such compounds are simply not able to occupy subpocket A because of the removal of the *N*-benzyl group. Such a modification leads to the loss of an essential aspect in the interactions with Bcl- x_L . In addition, we actually synthesized and tested a few compounds similar to those reported by Braud et al. by replacing the indole moiety with a substituted phenyl moiety (Schemes 1 and 2). The resulting compounds, BCL-LZH-23–26, were inactive against all three target proteins (Table 1). Considering the poor activities of these compounds and not to overlap with the compounds reported by Braud et al., we did not attempt to test more compounds of this type in our study.

The unsatisfactory activities of BCL-LZH-19–26 clearly indicates the importance of the *N*-benzyl-indole moiety, which is predicted to fill the hydrophobic subpocket A (Figure 2a). As the next step, we explored another two options, namely the use of 4-Et-Bn and 4-Ph-Bn as R^3 on this class of compound. The idea was to increase the size of R^3 to enhance the hydrophobic interactions with nearby residues on Bcl- x_L . The resulting compounds were BCL-LZH-27–43. The use of 4-Ph-Bn as R^3 was especially effective. The K_i values of a number of compounds were below 100 nm on Bcl- x_L (Table 1). In particular, the most potent compound (BCL-LZH-40) among them had a K_i value of 17 nm on Bcl- x_L , which was comparable to that of ABT-737. Note that BCL-LZH-40 also showed decent activities on Bcl-2 and Mcl-1 (K_i =534 nm and 200 nm, respectively).

The predicted binding mode of BCL-LZH-40 is shown in Figure 3. One can see that the overall binding mode of this compound is, not surprisingly, similar to that of BCL-LZH-02 (Figure 2a). Compared to BCL-LZH-02, BCL-LZH-40 has a considerably larger R^3 group, which results in enhanced hydrophobic interactions with subpocket A. The R^1 group on BCL-LZH-40–43 is simplified into an ethyl or methyl ester group; whereas the R^1 group on BCL-LZH-32–39 is still a phenylamide group like the template compound. Notably, the activities of BCL-LZH-32–39 on Bcl- x_L and Bcl-2 are generally comparable to those of BCL-LZH-40–43, but they are obviously less potent

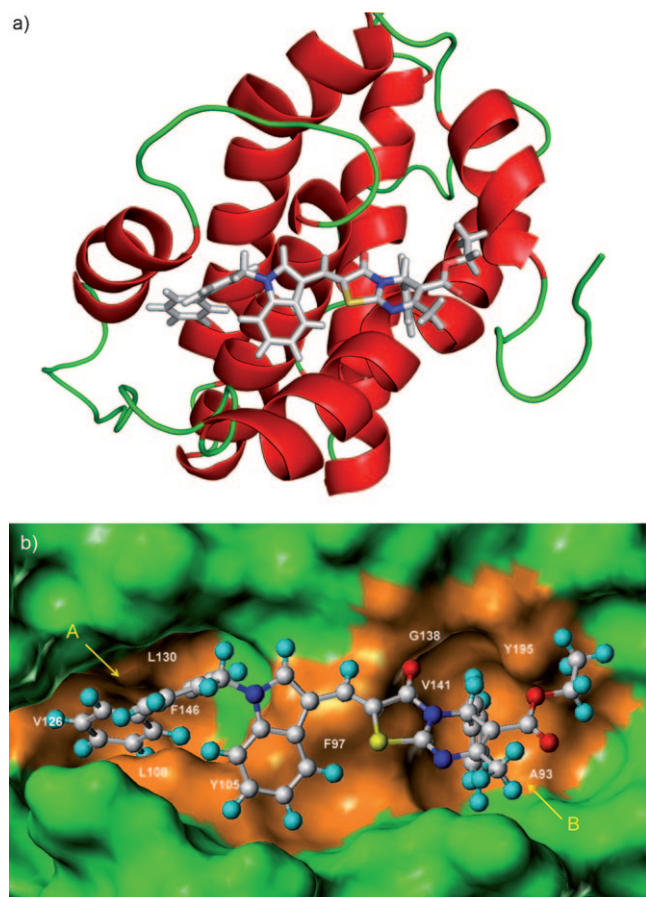


Figure 3. The binding mode of BCL-LZH-40 with Bcl- x_L as predicted by molecular docking and molecular dynamics simulation: a) the overall complex structure and b) the details at the binding site. Hydrophobic residues are colored in orange on the molecular surface of Bcl- x_L ; whereas other residues are colored in green.

on Mcl-1. In fact, the binding pocket on Mcl-1 where R^1 is supposed to locate is somewhat more restricted compared to that of Bcl- x_L or Bcl-2. Thus, one would expect that a less bulky R^1 group is more favorable for the binding of this class of compounds to Mcl-1.

Regarding Bcl-2, this class of compounds is generally less potent on Bcl-2 (Table 1) but the overall trend in the structure–activity relationship is similar to that on Bcl- x_L . As for Mcl-1, unfortunately the structure–activity relationship of our compounds is not obvious. In fact, the structure of Bcl-2 resembles that of Bcl- x_L whereas Mcl-1 has a somewhat different binding site. This may explain the different structure–activity relationships observed with Bcl- x_L /Bcl-2 and Mcl-1.

The absolute configuration of the chiral center on the dihydropyrimidine ring (Scheme 2) is, as yet, unresolved. So far we have not established an effective asymmetric synthetic method to obtain the pure *R* and *S* enantiomers of this class of compounds. Our attempts to crystallize several selected compounds were not very successful. All binding affinity data reported in this study are the results for racemic mixtures. According to our molecular modeling results, binding of the *R* enantiomer will differ from that of the *S* enantiomer in terms of

the orientation of the substituted phenyl R^2 group in subpocket B (see the Supporting Information). This difference does not change the overall binding mode of this class of compounds. Nevertheless, pure enantiomers may exhibit somewhat different structure–activity relationships regarding the role of R^2 . However, this speculation can be confirmed only after the samples of pure *R* and *S* enantiomers are obtained.

Conclusions

We have discovered and developed a class of compounds with a common thiazolo[3,2-*a*]pyrimidinone motif as general inhibitors of Bcl-2 family proteins. A total of 43 compounds were synthesized and tested against three Bcl-2 family proteins in an in vitro binding assay. A preliminary structure–activity relationship for this class of compounds was derived, which can be reasonably interpreted by molecular modeling results. Encouragingly, a number of compounds exhibited much improved binding affinities to the target proteins than the lead compound. The most potent compound among them, BCL-LZH-40, achieved tight binding to Bcl- x_L ($K_i = 17$ nM) comparable to ABT-737 ($K_i = 18$ nM). It is also a good binder to Mcl-1 ($K_i = 200$ nM) whereas ABT-737 is not. The true pharmaceutical value of this class of compounds remains to be explored using appropriate cell lines and animal models. Nevertheless, they are, at the very least, good binders to Bcl-2 family proteins at the molecular level. A practical advantage of this class of compounds is that their synthesis is relatively simple, and substituent groups can be conveniently introduced onto different sites. They may serve as a promising starting point for developing even more potent compounds that exhibit antitumor efficacy in vivo.

Experimental Section

Chemistry

Chemical reagents, solvents, and silica gel were obtained from commercial sources. They were used without further purification. Solvents were purified using standard procedures. For all compounds in this study, ^1H NMR spectra were recorded at 300 MHz on MERCURY300; ^{13}C NMR spectra were recorded at 100 MHz on a DPX-400 spectrometer. All NMR spectra were obtained in CDCl_3 or $[\text{D}_6]\text{DMSO}$, and results were recorded as parts per million (ppm) downfield from tetramethylsilane (TMS). The following abbreviations are used for multiplicity of NMR signals: s=singlet, d=doublet, t=triplet, q=quartet, m=multiplet, dd=double doublet, dt=double triplet, dq=double quartet, br=broad. High-resolution mass spectra (HRMS) were run on a HP5989A or VG Quattro MS/MS mass spectrometer. Purity of the compounds was determined via HPLC using a Perkin Elmer LC with PerkinElmer Series 200 Pump, PerkinElmer Series 200 UV/VIS Detector and Kromasil C18 column (4.5 mm \times 150 mm, 5 μm). Detection was conducted at 254 nm. The system conditions were CH_3OH (0.1% TFA) / H_2O (0.1% TFA), 80% (v/v) of CH_3OH gradient, flow rate: 1.0 mL min^{-1} (method A); CH_3OH (0.1% TFA) / H_2O (0.1% TFA), 10% (v/v) of CH_3OH at 0 to 10 min, 100% (v/v) of CH_3OH gradient at 10 to 20 min, 100% (v/v) of CH_3OH when longer than 20 min (method B).

ABT-737: This compound is a well-known small-molecule inhibitor of Bcl-2 family proteins originally developed by the Abbott Lab. It was used as a positive control in our study. A sample of this compound was provided by Shanghai ChemPartner Inc. The purity of the sample was 97.5% (t_R = 3.46 min) as determined by using an ACQUITY UPLC[®] System with an ACQUITY UPLC C18 column (2.1 mm × 50 mm, 1.7 μm). Optical detection was conducted at 254 nm. The mobile phase was a mixture of 0.02% TFA/H₂O and 0.02% TFA/MeCN with a flow rate of 0.65 mL min⁻¹. The detailed spectral data of this compound are listed below. ¹H NMR (300 MHz, [D₆]DMSO): δ = 8.46 (d, J = 1.5 Hz, 1H), 8.32 (s, 1H), 8.19 (d, J = 5.1 Hz, 1H), 7.80 (d, J = 4.8 Hz, 1H), 7.72 (d, J = 5.4 Hz, 2H), 7.53–7.48 (m, 5H), 7.37–7.23 (m, 8H), 6.90 (d, J = 4.8 Hz, 1H), 6.80 (d, J = 5.1 Hz, 2H), 4.08–4.00 (m, 1H), 3.38–3.34 (m, 4H), 3.14 (s, 4H), 3.05–2.96 (m, 2H), 2.64 (s, 6H), 2.39 (s, 4H), 2.09 (br s, 2H); ¹³C NMR (100 MHz, [D₆]DMSO): δ = 169.1, 152.3, 145.3, 140.8, 139.7, 135.1, 134.8, 131.9, 131.1, 130.1, 129.9, 129.7, 129.6, 129.0, 127.9, 127.4, 127.2, 126.2, 125.9, 113.7, 113.2, 79.2, 59.3, 54.0, 52.1, 50.3, 47.4, 42.7, 37.3, 30.7, 28.8 ppm; MS (ESI⁺): m/z (%): 813 [M+H]⁺ (100%); HRMS (MALDI): m/z calcd for C₄₂H₄₆N₆O₅S₂Cl [M+H]⁺: 813.2654, found: 813.2661.

(Z)-2-((1-(2-Fluorobenzyl)indol-3-yl)methylene)-5-(4-fluorophenyl)-7-methyl-3-oxo-*N*-phenylthiazolo[3,2-*a*]pyrimidine-6-carboxamide (BCL-LZH-01): (SPECS ID = AH-487/40936177). ¹H NMR (300 MHz, [D₆]DMSO): δ = 10.01 (s, 1H), 8.02 (d, J = 6.9 Hz, 2H), 7.92 (d, J = 7.2 Hz, 1H), 7.56 (t, J = 9.0 Hz, 3H), 7.38–7.15 (m, 12H), 7.05 (t, J = 7.5 Hz, 1H), 6.23 (s, 1H), 5.68 (s, 2H), 2.13 (s, 3H); ¹³C NMR (100 MHz, CDCl₃): δ = 165.6, 165.1, 163.8, 162.0, 161.4, 159.5, 157.5, 153.4, 141.6, 139.3, 136.7, 132.3, 130.9, 130.4, 130.0, 129.4, 128.0, 125.5, 124.6, 124.4, 124.2, 122.3, 120.4, 119.6, 116.4, 115.0, 113.7, 111.7, 111.0, 56.1, 44.7, 21.9 ppm; MS (ESI): m/z (%): 617.1 [M+H]⁺ (100%), 639.1 [M+Na]⁺ (12%); HRMS (MALDI): m/z calcd for C₃₆H₂₇N₄O₄F₂S [M+H]⁺: 617.1817, found: 617.1811; HPLC (method A): t_R = 19.45 min (92.3%).

Preparation of BCL-LZH thiazolo[3,2-*a*]pyrimidinone compounds (general procedure A): Biginelli product **3** (0.33 mmol) and substituted aldehyde **4** (0.33 mmol) added to a stirred mixture of 2-chloroacetic acid (33 mg, 0.35 mmol), sodium acetate (200 mg, 2.44 mmol), acetic acid (1.00 mL) and acetic anhydride (0.50 mL) at RT. The mixture was brought to 80 °C, maintained for 24 h and then cooled to RT. Water was added to quench the reaction. The mixture was diluted with CH₂Cl₂, washed with water, brine, and the aqueous phase was then extracted with CH₂Cl₂ (3 × 50 mL). The combined organic phase was washed with brine, dried (Na₂SO₄), filtered, and evaporated. The crude reaction mixture was purified by flash chromatography (silica gel, CH₂Cl₂/THF) to afford thiazolo[3,2-*a*]pyrimidinone compounds BCL-LZH-02–43.

(Z)-2-((1-Benzyl-indol-3-yl)methylene)-7-methyl-3-oxo-*N*,5-diphenylthiazolo[3,2-*a*]pyrimidine-6-carboxamide (BCL-LZH-02): General procedure A afforded BCL-LZH-02 as a yellow solid (33 mg, 17%). ¹H NMR (300 MHz, [D₆]DMSO): δ = 10.03 (s, 1H), 8.11 (s, 1H), 8.03 (s, 1H), 7.91 (d, J = 7.2 Hz, 1H), 7.56 (dd, J = 7.8, 1.5 Hz, 3H), 7.38–7.17 (m, 14H), 7.05 (t, J = 7.5 Hz, 1H), 6.24 (s, 1H), 5.61 (s, 2H), 2.13 ppm (d, J = 0.6 Hz, 3H); ¹³C NMR (100 MHz, CDCl₃): δ = 165.3, 154.8, 143.5, 139.7, 137.5, 136.7, 135.6, 130.3, 129.4, 129.3, 129.2, 129.0, 128.5, 128.1, 127.6, 127.3, 126.8, 124.9, 124.8, 123.9, 122.0, 120.1, 119.1, 113.9, 111.7, 110.6, 56.4, 51.1, 29.8, 21.9 ppm; MS (ESI): m/z (%): 581 [M+H]⁺ (100%), 603 [M+Na]⁺ (95%), 619 [M+K]⁺ (30%); HRMS (ESI): m/z calcd for C₃₆H₂₉N₄O₂S [M+H]⁺: 581.2006, found: 581.2015; HPLC (method A): t_R = 66.98 min (72.4%).

(Z)-2-((1-Benzyl-indol-3-yl)methylene)-5-(4-bromophenyl)-7-methyl-3-oxo-*N*-phenylthiazolo[3,2-*a*]pyrimidine-6-carboxamide

(BCL-LZH-03): General procedure A afforded BCL-LZH-03 as a yellow solid (20 mg, 9%). ¹H NMR (300 MHz, [D₆]DMSO): δ = 10.04 (s, 1H), 8.12 (s, 1H), 8.03 (s, 1H), 8.98–8.90 (m, 1H), 7.63–7.18 (m, 16H), 7.06 (t, J = 7.5 Hz, 1H), 6.21 (s, 1H), 5.62 (s, 2H), 2.13 ppm (s, 3H); ¹³C NMR (100 MHz, [D₆]DMSO): δ = 164.9, 164.4, 152.8, 141.0, 139.1, 138.6, 137.0, 136.0, 131.7, 129.1, 128.7, 127.7, 127.5, 127.2, 124.1, 123.7, 121.6, 121.5, 119.8, 118.8, 113.9, 112.7, 111.3, 110.2, 55.5, 49.8, 21.3 ppm; MS (MALDI): m/z (%): 659 [M+H]⁺ (100%), 681 [M+Na]⁺ (95%); HRMS (ESI): m/z calcd for C₃₆H₂₈BrN₄O₂S [M+H]⁺: 659.1111, found: 659.1121; HPLC (method A): t_R = 7.60 min (97.5%).

(Z)-2-((1-Benzyl-indol-3-yl)methylene)-5-(4-methoxyphenyl)-7-methyl-3-oxo-*N*-phenylthiazolo[3,2-*a*]pyrimidine-6-carboxamide (BCL-LZH-04): General procedure A afforded BCL-LZH-04 as a yellow solid (7 mg, 3%). ¹H NMR (300 MHz, [D₆]DMSO): δ = 10.02 (s, 1H), 8.10 (s, 1H), 8.02 (s, 1H), 7.91 (d, J = 8.4 Hz, 1H), 7.57 (d, J = 7.5 Hz, 3H), 7.34–7.19 (m, 11H), 7.05 (t, J = 7.5 Hz, 1H), 6.90 (d, J = 8.4 Hz, 2H), 6.19 (s, 1H), 5.61 (s, 2H), 3.69 (d, J = 2.7 Hz, 3H), 2.14 ppm (s, 3H); ¹³C NMR (100 MHz, CDCl₃): δ = 165.4, 165.3, 160.1, 154.6, 143.6, 137.6, 136.6, 135.6, 131.6, 130.3, 129.2, 129.1, 129.0, 128.9, 128.3, 128.0, 127.2, 124.8, 124.6, 123.8, 121.9, 120.1, 119.0, 114.6, 114.5, 113.8, 111.5, 110.6, 55.8, 55.3, 50.9, 21.7 ppm; MS (ESI): m/z (%): 611 [M+H]⁺ (100%); HRMS (ESI): m/z calcd for C₃₇H₃₁N₄O₃S [M+H]⁺: 611.2111, found: 611.2109; HPLC (method A): t_R = 22.49 min (79.0%).

(Z)-2-((1-Benzyl-indol-3-yl)methylene)-5-(4-ethylphenyl)-7-methyl-3-oxo-*N*-phenylthiazolo[3,2-*a*]pyrimidine-6-carboxamide (BCL-LZH-05): General procedure A afforded BCL-LZH-05 as a yellow solid (16 mg, 8%). ¹H NMR (300 MHz, [D₆]DMSO): δ = 10.03 (s, 1H), 8.10 (s, 1H), 8.03 (s, 1H), 7.93–7.89 (m, 1H), 7.57 (dd, J = 8.1, 2.1 Hz, 3H), 7.37–7.17 (m, 13H), 7.05 (t, J = 7.5 Hz, 1H), 6.21 (s, 1H), 5.61 (s, 2H), 2.54 (q, J = 7.5 Hz, 2H), 2.13 (s, 3H), 1.12 ppm (t, J = 7.5 Hz, 3H); ¹³C NMR (100 MHz, CDCl₃): δ = 165.4, 165.3, 154.7, 145.3, 143.6, 137.6, 136.8, 136.6, 135.6, 130.2, 129.1, 129.0, 128.8, 128.4, 128.0, 127.6, 127.2, 124.8, 124.6, 123.8, 121.9, 120.1, 119.0, 113.8, 113.7, 111.6, 110.6, 56.1, 51.0, 28.6, 21.8, 15.3 ppm; MS (ESI): m/z (%): 609 [M+H]⁺ (100%), 631 [M+Na]⁺ (35%); HRMS (ESI): m/z calcd for C₃₈H₃₃N₄O₂S [M+H]⁺: 609.2319, found: 609.2333; HPLC (method A): t_R = 23.17 min (83.4%).

(Z)-3-(2-((1-Benzyl-indol-3-yl)methylene)-7-methyl-3-oxo-6-(phenylcarbamoyl)thiazolo[3,2-*a*]pyrimidin-5-yl)phenyl acetate (BCL-LZH-06): General procedure A afforded BCL-LZH-06 as a yellow solid (82 mg, 39%). ¹H NMR (300 MHz, [D₆]DMSO): δ = 10.03 (s, 0.8H), 9.98 (s, 0.2H), 8.11 (s, 1H), 8.05 (s, 1H), 7.95–7.90 (m, 1H), 7.58–7.53 (m, 3H), 7.42–7.18 (m, 11H), 7.10–6.97 (m, 3H), 6.25 (s, 1H), 5.61 (s, 1.7H), 5.57 (s, 0.3H), 2.23 (s, 3H), 2.13 (s, 2.5H), 2.09 ppm (s, 0.5H); ¹³C NMR (100 MHz, CDCl₃): δ = 169.4, 165.4, 165.1, 154.4, 151.3, 142.2, 140.9, 137.5, 136.6, 135.6, 130.3, 130.1, 129.1, 129.0, 128.4, 128.0, 127.2, 125.4, 125.0, 124.7, 123.8, 122.2, 121.9, 120.9, 120.3, 119.1, 114.1, 113.5, 111.6, 110.5, 55.9, 50.9, 21.5, 21.2 ppm; MS (ESI): m/z (%): 639 [M+H]⁺ (100%), 661 [M+Na]⁺ (75%); HRMS (MALDI): m/z calcd for C₃₈H₃₁N₄O₄S [M+H]⁺: 639.2061, found: 639.2058; HPLC (method B): t_R = 13.27 min (94.3%).

(Z)-4-(2-((1-Benzyl-indol-3-yl)methylene)-7-methyl-3-oxo-6-(phenylcarbamoyl)thiazolo[3,2-*a*]pyrimidin-5-yl)phenyl acetate (BCL-LZH-07): General procedure A afforded BCL-LZH-07 as a yellow solid (61 mg, 29%). ¹H NMR (300 MHz, [D₆]DMSO): δ = 10.04 (s, 1H), 8.10 (s, 1H), 8.05 (s, 1H), 7.92 (dd, J = 7.5, 0.9 Hz, 1H), 7.56 (dd, J = 7.5, 2.7 Hz, 3H), 7.37–7.18 (m, 11H), 7.14–7.03 (m, 3H), 6.25 (s, 1H), 5.61 (s, 2H), 2.23 (s, 3H), 2.13 ppm (d, J = 0.9 Hz, 3H);

^{13}C NMR (100 MHz, $[\text{D}_6]\text{DMSO}$): δ = 169.1, 165.0, 164.5, 152.9, 150.3, 141.0, 138.7, 137.3, 137.0, 136.1, 131.7, 128.7, 128.7, 128.0, 127.7, 127.5, 127.3, 124.2, 123.7, 123.4, 122.2, 121.5, 119.8, 118.9, 114.3, 112.8, 111.3, 110.2, 55.4, 49.8, 21.3, 20.8 ppm; MS (ESI): m/z (%): 639 $[\text{M}+\text{H}]^+$ (23%), 661 $[\text{M}+\text{Na}]^+$ (100%), 677 $[\text{M}+\text{K}]^+$ (27%); HRMS (MALDI): m/z calcd for $\text{C}_{38}\text{H}_{31}\text{N}_4\text{O}_5\text{S}$ $[\text{M}+\text{H}]^+$: 639.2066, found: 639.2061; HPLC (method B): t_{R} = 13.39 min (65.6%).

(Z)-4-(2-((1-Benzyl-indol-3-yl)methylene)-7-methyl-3-oxo-6-(phenylcarbamoyl)thiazolo[3,2-*a*]pyrimidin-5-yl)-1,2-phenylene diacetate (BCL-LZH-08): General procedure A afforded BCL-LZH-08 as a yellow solid (51 mg, 22%). ^1H NMR (300 MHz, $[\text{D}_6]\text{DMSO}$): δ = 10.06 (s, 1H), 8.12 (s, 1H), 8.07 (s, 1H), 7.93 (d, J = 7.5 Hz, 1H), 7.56 (t, J = 6.9 Hz, 3H), 7.37–7.16 (m, 12H), 7.07 (t, J = 7.5 Hz, 1H), 6.26 (s, 1H), 5.62 (s, 2H), 2.24 (d, J = 1.5 Hz, 6H), 2.14 ppm (s, 3H); ^{13}C NMR (100 MHz, CDCl_3): δ = 168.4, 168.1, 165.5, 165.2, 154.4, 142.6, 142.5, 142.0, 137.9, 137.4, 136.7, 135.7, 130.4, 129.2, 129.1, 129.0, 129.0, 128.5, 128.1, 127.3, 126.8, 126.4, 125.2, 124.8, 124.0, 123.9, 123.0, 122.0, 120.5, 119.2, 114.2, 113.6, 111.7, 110.6, 55.5, 51.1, 21.5, 20.9, 20.7 ppm; MS (ESI): m/z (%): 697 $[\text{M}+\text{H}]^+$ (15%), 719 $[\text{M}+\text{Na}]^+$ (100%), 735 $[\text{M}+\text{K}]^+$ (11%); HRMS (MALDI): m/z calcd for $\text{C}_{40}\text{H}_{33}\text{N}_4\text{O}_6\text{S}$ $[\text{M}+\text{H}]^+$: 697.2121, found: 697.2115; HPLC (method A): t_{R} = 10.99 min (95.0%).

(Z)-Ethyl 2-((1-Benzyl-indol-3-yl)methylene)-7-methyl-3-oxo-5-phenylthiazolo[3,2-*a*]pyrimidine-6-carboxylate (BCL-LZH-09): General procedure A afforded BCL-LZH-09 as a yellow solid (73 mg, 42%). ^1H NMR (300 MHz, CDCl_3): δ = 8.09 (s, 1H), 7.78 (dd, J = 6.3, 3.0 Hz, 1H), 7.43 (dd, J = 7.8, 1.5 Hz, 2H), 7.39 (s, 1H), 7.35–6.83 (m, 11H), 6.21 (s, 1H), 5.38 (s, 2H), 4.10 (q, J = 6.9 Hz, 2H), 2.52 (s, 3H), 1.19 ppm (t, J = 7.2 Hz, 3H); ^{13}C NMR (100 MHz, CDCl_3): δ = 165.7, 165.3, 156.7, 152.8, 140.5, 136.6, 135.6, 130.3, 129.2, 128.6, 128.4, 128.1, 127.2, 125.2, 123.9, 121.9, 119.0, 114.0, 111.6, 110.5, 108.6, 60.5, 55.4, 51.0, 22.9, 14.2 ppm; MS (ESI): m/z (%): 534 $[\text{M}+\text{H}]^+$ (100%), 556 $[\text{M}+\text{Na}]^+$ (27%); HRMS (ESI): m/z calcd for $\text{C}_{32}\text{H}_{26}\text{N}_3\text{O}_3\text{S}$ $[\text{M}+\text{H}]^+$: 534.1846, found: 534.1859; HPLC (method A): t_{R} = 19.45 min (72.3%).

(Z)-Ethyl 2-((1-Benzyl-indol-3-yl)methylene)-5-(3-chlorophenyl)-7-methyl-3-oxo-thiazolo[3,2-*a*]pyrimidine-6-carboxylate (BCL-LZH-10): General procedure A afforded BCL-LZH-10 as a yellow solid (84 mg, 45%). ^1H NMR (300 MHz, CDCl_3): δ = 9.97 (s, 0.4H), 8.33–8.30 (m, 0.4H), 8.07 (s, 0.6H), 7.76–7.74 (m, 0.6H), 7.68 (s, 0.4H), 7.43–7.04 (m, 13H), 6.12–6.08 (m, 0.6H), 5.43–5.26 (m, 2H), 4.17–4.01 (m, 2H), 2.52–2.35 (m, 3H), 1.26–1.09 ppm (m, 3H); ^{13}C NMR (100 MHz, CDCl_3): δ = 165.5, 165.2, 156.7, 153.4, 142.4, 136.7, 135.5, 134.5, 130.4, 129.9, 129.2, 128.9, 128.5, 128.3, 128.1, 127.3, 126.4, 125.6, 124.0, 122.1, 119.1, 113.7, 111.6, 110.6, 108.0, 60.6, 55.0, 51.1, 23.0, 14.2 ppm; MS (ESI): m/z (%): 568 $[\text{M}+\text{H}]^+$ (100%); HRMS (MALDI): m/z calcd for $\text{C}_{32}\text{H}_{27}\text{ClN}_3\text{O}_3\text{S}$ $[\text{M}+\text{H}]^+$: 568.1456, found: 568.1460; HPLC (method B): t_{R} = 11.42 min (74.3%).

(Z)-Ethyl 2-((1-Benzyl-indol-3-yl)methylene)-5-(3-methoxyphenyl)-7-methyl-3-oxo-thiazolo[3,2-*a*]pyrimidine-6-carboxylate (BCL-LZH-11): General procedure A afforded BCL-LZH-11 as a yellow solid (57 mg, 31%). ^1H NMR (300 MHz, CDCl_3): δ = 8.07 (s, 1H), 7.77–7.74 (m, 1H), 7.36–7.14 (m, 10H), 7.02–6.97 (m, 2H), 6.78 (dd, J = 8.1, 1.8 Hz, 1H), 6.16 (s, 1H), 5.34 (s, 2H), 4.12 (q, J = 6.9 Hz, 2H), 3.76 (s, 3H), 2.51 (s, 3H), 1.21 ppm (t, J = 7.2 Hz, 3H); ^{13}C NMR (100 MHz, CDCl_3): δ = 165.6, 165.1, 159.6, 156.5, 152.7, 141.8, 136.5, 135.4, 130.1, 129.5, 129.0, 128.3, 127.9, 127.1, 125.0, 123.7, 121.8, 120.1, 118.9, 113.9, 113.7, 111.4, 110.4, 108.3, 60.3, 55.1, 50.8, 22.7, 14.1 ppm; MS (ESI): m/z (%): 564 $[\text{M}+\text{H}]^+$ (100%), 586 $[\text{M}+\text{Na}]^+$ (10%); HRMS (MALDI): m/z calcd for $\text{C}_{33}\text{H}_{30}\text{N}_3\text{O}_4\text{S}$ $[\text{M}+\text{H}]^+$:

564.1952, found: 564.1957; HPLC (method B): t_{R} = 15.15 min (60.6%).

(Z)-Ethyl 2-((1-Benzyl-indol-3-yl)methylene)-5-(4-ethylphenyl)-7-methyl-3-oxothiazolo[3,2-*a*]pyrimidine-6-carboxylate (BCL-LZH-12): General procedure A afforded BCL-LZH-12 as a yellow solid (35 mg, 19%). ^1H NMR (300 MHz, CDCl_3): δ = 8.09 (s, 1H), 7.78 (dd, J = 6.0, 1.8 Hz, 1H), 7.38 (s, 1H), 7.35–7.10 (m, 12H), 6.18 (s, 1H), 5.38 (s, 2H), 4.11 (q, J = 7.2 Hz, 2H), 2.59 (q, J = 7.8 Hz, 2H), 2.51 (s, 3H), 1.23–1.15 ppm (m, 6H); ^{13}C NMR (100 MHz, CDCl_3): δ = 165.7, 165.1, 156.5, 152.5, 144.5, 137.8, 136.5, 135.5, 130.1, 129.0, 128.3, 128.0, 127.9, 127.2, 124.8, 123.7, 121.8, 118.8, 113.9, 111.4, 110.4, 108.6, 60.3, 55.1, 50.8, 28.5, 22.8, 15.3, 14.1 ppm; MS (ESI): m/z (%): 562 $[\text{M}+\text{H}]^+$ (100%); HRMS (ESI): m/z calcd for $\text{C}_{34}\text{H}_{32}\text{N}_3\text{O}_3\text{S}$ $[\text{M}+\text{H}]^+$: 562.2159, found: 562.2169; HPLC (method B): t_{R} = 15.89 min (78.0%).

(Z)-2-((1-Benzyl-indol-3-yl)methylene)-N,7-dimethyl-3-oxo-N,5-diphenylthiazolo[3,2-*a*]pyrimidine-6-carboxamide (BCL-LZH-13): General procedure A afforded BCL-LZH-13 as a yellow solid (44 mg, 22%). ^1H NMR (300 MHz, CDCl_3): δ = 8.01 (s, 1H), 7.74 (dd, J = 6.9, 2.1 Hz, 1H), 7.39–7.16 (m, 17H), 6.84 (s, 2H), 5.88 (s, 1H), 5.37 (s, 2H), 3.16 (s, 3H), 1.98 ppm (s, 3H); ^{13}C NMR (100 MHz, CDCl_3): δ = 165.1, 139.6, 136.6, 135.6, 130.0, 129.3, 129.1, 128.8, 128.4, 128.1, 127.2, 127.1, 126.0, 124.2, 123.8, 121.8, 119.0, 113.9, 111.6, 110.5, 68.0, 51.0, 38.0, 25.7 ppm; MS (ESI): m/z (%): 595 $[\text{M}+\text{H}]^+$ (100%), 617 $[\text{M}+\text{Na}]^+$ (13%); HRMS (MALDI): m/z calcd for $\text{C}_{37}\text{H}_{31}\text{N}_4\text{O}_3\text{S}$ $[\text{M}+\text{H}]^+$: 595.2162, found: 595.2163; HPLC (method A): t_{R} = 22.55 min (93.9%).

(Z)-2-((1-Benzyl-indol-3-yl)methylene)-N,7-dimethyl-3-oxo-5-phenylthiazolo[3,2-*a*]pyrimidine-6-carboxamide (BCL-LZH-14): General procedure A afforded BCL-LZH-14 as a yellow solid (61 mg, 36%). ^1H NMR (300 MHz, $[\text{D}_6]\text{DMSO}$): δ = 8.99 (s, 0.1H), 8.06 (s, 0.9H), 8.00 (s, 2H), 7.87 (d, J = 7.2 Hz, 1H), 7.54 (d, J = 8.1 Hz, 1H), 7.37–7.16 (m, 12H), 6.12 (s, 1H), 5.59 (s, 1.8H), 5.54 (s, 0.2H), 2.58 (d, J = 4.2 Hz, 3H), 2.08 (s, 2.7H), 2.04 ppm (s, 0.3H); ^{13}C NMR (100 MHz, $[\text{D}_6]\text{DMSO}$): δ = 166.5, 164.4, 152.3, 139.9, 139.8, 137.0, 136.0, 131.5, 128.7, 128.3, 127.7, 127.4, 127.2, 126.7, 123.6, 123.3, 121.4, 118.8, 114.3, 113.0, 111.3, 110.2, 55.7, 49.8, 25.7, 21.1 ppm; MS (ESI): m/z (%): 519 $[\text{M}+\text{H}]^+$ (100%), 541 $[\text{M}+\text{Na}]^+$ (18%); HRMS (MALDI): m/z calcd for $\text{C}_{31}\text{H}_{27}\text{N}_4\text{O}_2\text{S}$ $[\text{M}+\text{H}]^+$: 519.1849, found: 519.1846; HPLC (method A): t_{R} = 26.16 min (69.8%).

(Z)-Methyl 2-((1-Benzyl-indol-3-yl)methylene)-7-methyl-3-oxo-5-phenylthiazolo[3,2-*a*]pyrimidine-6-carboxylate (BCL-LZH-15): General procedure A afforded BCL-LZH-15 as a yellow solid (20 mg, 12%). ^1H NMR (300 MHz, CDCl_3): δ = 8.08 (s, 1H), 7.77 (d, J = 8.1 Hz, 1H), 7.44–7.07 (m, 14H), 6.21 (s, 1H), 5.36–5.29 (m, 2H), 3.67–3.57 (m, 3H), 2.52–2.50 ppm (m, 3H); ^{13}C NMR (100 MHz, CDCl_3): δ = 166.1, 165.2, 156.7, 140.3, 136.5, 135.4, 130.2, 129.1, 128.9, 128.8, 128.6, 128.5, 128.3, 128.2, 127.9, 127.8, 127.7, 127.1, 126.8, 126.5, 125.2, 125.1, 123.8, 121.8, 118.9, 113.8, 111.4, 110.4, 108.2, 55.2, 51.4, 50.9, 22.9 ppm; MS (ESI): m/z (%): 520 $[\text{M}+\text{H}]^+$ (100%), 558 $[\text{M}+\text{K}]^+$ (5%); HRMS (MALDI): m/z calcd for $\text{C}_{31}\text{H}_{26}\text{N}_3\text{O}_3\text{S}$ $[\text{M}+\text{H}]^+$: 520.1689, found: 520.1691; HPLC (method A): t_{R} = 24.95 min (40.7%).

(Z)-4-(2-((1-Benzylindol-3-yl)methylene)-7-methyl-6-(methyl(phenyl)carbamoyl)-3-oxothiazolo[3,2-*a*]pyrimidin-5-yl)phenyl acetate (BCL-LZH-16): General procedure A afforded BCL-LZH-16 as a yellow solid (42 mg, 19%). ^1H NMR (300 MHz, CDCl_3): δ = 8.00 (s, 1H), 7.74 (d, J = 6.9 Hz, 1H), 7.35–7.07 (m, 16H), 6.79 (br s, 2H), 5.92 (br s, 1H), 5.35 (s, 2H), 3.19 (br s, 3H), 2.28 (s, 3H), 1.98 ppm (s, 3H); ^{13}C NMR (100 MHz, CDCl_3): δ = 169.1, 168.3, 164.9, 153.3, 150.8, 142.8, 136.9, 136.4, 135.5, 129.9, 129.2, 129.0, 128.8, 128.2, 127.9,

127.1, 126.5, 125.9, 124.2, 123.6, 122.1, 121.7, 118.9, 113.7, 113.2, 111.4, 110.3, 56.4, 50.8, 37.9, 21.3, 21.0 ppm; MS (ESI): m/z (%): 653 $[M+H]^+$ (88%), 675 $[M+Na]^+$ (100%), 691 $[M+K]^+$ (15%); HRMS (MALDI): m/z calcd for $C_{39}H_{33}N_4O_4S$ $[M+H]^+$: 653.2217, found: 653.2211; HPLC (method B): t_R = 13.39 min (94.4%).

(Z)-4-(2-((1-Benzylindol-3-yl)methylene)-7-methyl-6-(methylcarbamoyl)-3-oxothiazolo[3,2-*a*]pyrimidin-5-yl)phenyl acetate (BCL-LZH-17): General procedure A afforded BCL-LZH-17 as a yellow solid (99 mg, 52%). 1H NMR (300 MHz, $CDCl_3$): δ = 8.03 (s, 1H), 7.75 (dd, J = 6.3, 2.4 Hz, 1H), 7.41–6.99 (m, 13H), 6.14 (s, 1H), 5.54 (d, J = 5.1 Hz, 1H), 5.35 (s, 2H), 2.75 (d, J = 4.5 Hz, 3H), 2.28–2.19 ppm (m, 6H); ^{13}C NMR (100 MHz, $CDCl_3$): δ = 169.3, 167.8, 165.3, 154.3, 151.0, 141.8, 137.2, 136.7, 135.7, 130.3, 129.2, 128.7, 128.4, 128.2, 127.3, 124.8, 123.9, 122.2, 121.9, 119.2, 113.9, 111.7, 110.6, 55.7, 51.1, 29.8, 26.6, 21.7, 21.3 ppm; MS (ESI): m/z (%): 577 $[M+H]^+$ (100%), 599 $[M+Na]^+$ (60%); HRMS (ESI): m/z calcd for $C_{33}H_{29}N_4O_4S$ $[M+H]^+$: 577.1904, found: 577.1911; HPLC (method A): t_R = 21.22 min (85.3%).

(Z)-Methyl 5-(4-acetoxyphenyl)-2-((1-benzylindol-3-yl)methylene)-7-methyl-3-oxothiazolo[3,2-*a*]pyrimidine-6-carboxylate (BCL-LZH-18): General procedure A afforded BCL-LZH-18 as a yellow solid (115 mg, 60%). 1H NMR (300 MHz, $CDCl_3$): δ = 8.09 (s, 1H), 7.79–7.76 (m, 1H), 7.46–7.15 (m, 12H), 7.03 (d, J = 8.4 Hz, 2H), 6.22 (s, 1H), 5.37 (s, 2H), 3.67 (s, 3H), 2.52 (s, 3H), 2.26 ppm (s, 3H); ^{13}C NMR (100 MHz, $CDCl_3$): δ = 169.2, 166.0, 165.1, 156.7, 153.4, 150.6, 137.8, 136.5, 135.4, 130.3, 129.0, 128.9, 128.3, 127.9, 127.1, 126.6, 125.4, 123.8, 121.9, 121.6, 118.9, 113.7, 111.4, 110.4, 107.9, 54.4, 51.5, 50.9, 22.9, 21.1 ppm; MS (ESI): m/z (%): 578 $[M+H]^+$ (100%), 600 $[M+Na]^+$ (22%); HRMS (ESI): m/z calcd for $C_{33}H_{28}N_3O_5S$ $[M+H]^+$: 578.1744, found: 578.1751; HPLC (method A): t_R = 21.33 min (97.1%).

(Z)-7-Methyl-2-((1-methylindol-3-yl)methylene)-3-oxo-*N*,5-diphenylthiazolo[3,2-*a*]pyrimidine-6-carboxamide (BCL-LZH-19): General procedure A afforded BCL-LZH-19 as a yellow solid (86 mg, 52%). 1H NMR (300 MHz, $[D_6]DMSO$): δ = 10.04 (s, 1H), 8.01 (s, 1H), 7.90–7.87 (m, 2H), 7.58–7.54 (m, 3H), 7.38–7.19 (m, 9H), 7.05 (t, J = 7.5 Hz, 1H), 6.24 (s, 1H), 3.94–3.87 (m, 3H), 2.18–2.09 ppm (m, 3H); ^{13}C NMR (100 MHz, $[D_6]DMSO$): δ = 169.3, 168.4, 165.1, 162.8, 156.7, 153.0, 145.9, 140.7, 140.4, 138.8, 136.3, 135.9, 128.9, 128.8, 128.6, 128.4, 128.2, 128.1, 126.8, 126.3, 123.5, 122.8, 121.4, 121.3, 119.7, 118.9, 118.2, 113.7, 112.1, 111.2, 110.7, 104.5, 55.7, 33.3, 21.2 ppm; MS (ESI): m/z (%): 505 $[M+H]^+$ (100%), 527 $[M+Na]^+$ (9%); HRMS (MALDI): m/z calcd for $C_{30}H_{25}N_4O_2S$ $[M+H]^+$: 505.1693, found: 505.1683; HPLC (method B): t_R = 13.15 min (81.8%).

(Z)-3-(7-Methyl-2-((1-methylindol-3-yl)methylene)-3-oxo-6-(phenylcarbamoyl)thiazolo[3,2-*a*]pyrimidin-5-yl)phenyl acetate (BCL-LZH-20): General procedure A afforded BCL-LZH-20 as a yellow solid (66 mg, 36%). 1H NMR (300 MHz, $[D_6]DMSO$): δ = 10.02 (s, 0.9H), 9.98 (s, 0.1H), 8.04 (s, 1H), 7.92–7.89 (m, 2H), 7.59–7.53 (m, 3H), 7.40 (t, J = 7.8 Hz, 1H), 7.35–7.18 (m, 5H), 7.10–7.01 (m, 3H), 6.24 (s, 1H), 3.95 (s, 2.7H), 3.89 (s, 0.3H), 2.23 (s, 3H), 2.14 (s, 2.7H), 2.09 ppm (s, 0.3H); ^{13}C NMR (100 MHz, $[D_6]DMSO$): δ = 168.9, 164.9, 164.4, 153.0, 150.7, 141.4, 141.3, 138.6, 136.8, 132.4, 129.8, 128.6, 127.2, 124.3, 123.7, 123.2, 122.1, 121.4, 119.9, 11.08, 109.5, 55.5, 33.3, 21.3, 20.8 ppm; MS (ESI): m/z (%): 563 $[M+H]^+$ (55%), 585 $[M+Na]^+$ (100%), 601 $[M+K]^+$ (3%); HRMS (MALDI): m/z calcd for $C_{32}H_{27}N_4O_4S$ $[M+H]^+$: 563.1748, found: 563.1747; HPLC (method B): t_R = 12.90 min (93.9%).

(Z)-4-(7-Methyl-2-((1-methylindol-3-yl)methylene)-3-oxo-6-(phenylcarbamoyl)thiazolo[3,2-*a*]pyrimidin-5-yl)phenyl acetate (BCL-LZH-21): General procedure A afforded BCL-LZH-21 as a

yellow solid (71 mg, 38%). 1H NMR (300 MHz, $[D_6]DMSO$): δ = 10.03 (s, 0.9H), 10.00 (s, 0.1H), 8.03 (s, 1H), 7.92–7.88 (m, 2H), 7.59–7.54 (m, 3H), 7.34–7.21 (m, 6H), 7.13–7.03 (m, 3H), 6.25 (s, 1H), 3.95 (s, 2.7H), 3.89 (s, 0.3H), 2.23 (s, 3H), 2.14 (s, 2.7H), 2.09 ppm (s, 0.3H); ^{13}C NMR (100 MHz, $[D_6]DMSO$): δ = 169.0, 165.0, 164.5, 152.9, 150.3, 141.1, 138.6, 137.3, 136.8, 132.4, 128.6, 128.1, 127.2, 124.3, 123.7, 123.2, 122.2, 121.4, 119.8, 118.6, 114.2, 112.0, 110.8, 109.5, 67.0, 55.4, 33.4, 25.1, 21.3, 20.8 ppm; MS (ESI): m/z (%): 563 $[M+H]^+$ (73%), 585 $[M+Na]^+$ (100%), 601 $[M+K]^+$ (7%); HRMS (MALDI): m/z calcd for $C_{32}H_{27}N_4O_4S$ $[M+H]^+$: 563.1748, found: 563.1769; HPLC (method B): t_R = 12.83 min (96.1%).

(Z)-4-(7-Methyl-2-((1-methylindol-3-yl)methylene)-3-oxo-6-(phenylcarbamoyl)thiazolo[3,2-*a*]pyrimidin-5-yl)-1,2-phenylene diacetate (BCL-LZH-22): General procedure A afforded BCL-LZH-22 as a yellow solid (46 mg, 22%). R_f 0.17 (silica gel, CH_2Cl_2/THF 100:3); 1H NMR (300 MHz, $[D_6]DMSO$): δ = 10.04 (s, 0.8H), 10.01 (s, 0.2H), 8.05 (s, 1H), 7.94–7.90 (m, 2H), 7.59–7.53 (m, 3H), 7.35–7.21 (m, 6H), 7.16 (t, J = 1.8 Hz, 1H), 7.11–7.04 (m, 1H), 6.25 (s, 1H), 3.95 (s, 2.4H), 3.90 (s, 0.6H), 2.24 (s, 6H), 2.15 (s, 2.4H), 2.10 ppm (s, 0.6H); ^{13}C NMR (100 MHz, $[D_6]DMSO$): δ = 168.0, 167.9, 164.9, 164.4, 153.0, 142.0, 141.5, 138.6, 138.3, 136.8, 132.4, 128.6, 127.2, 125.2, 124.5, 124.1, 123.7, 123.2, 121.9, 121.4, 120.0, 118.6, 113.6, 111.8, 109.6, 55.1, 33.3, 21.4, 20.3 ppm; MS (ESI): m/z (%): 621 $[M+H]^+$ (55%), 643 $[M+Na]^+$ (100%), 659 $[M+K]^+$ (5%); HRMS (MALDI): m/z calcd for $C_{34}H_{29}N_4O_6S$ $[M+H]^+$: 621.1802, found: 621.1794; HPLC (method B): t_R = 12.73 min (90.8%).

(Z)-2-Benzylidene-7-methyl-3-oxo-*N*,5-diphenylthiazolo[3,2-*a*]pyrimidine-6-carboxamide (BCL-LZH-23): General procedure A afforded BCL-LZH-23 as a yellow solid (78 mg, 52%). 1H NMR (300 MHz, $[D_6]DMSO$): δ = 10.02 (s, 1H), 7.77 (s, 1H), 7.62 (d, J = 7.5 Hz, 2H), 7.56–7.46 (m, 5H), 7.38–7.25 (m, 7H), 7.05 (d, J = 7.5 Hz, 1H), 6.23 (s, 1H), 2.13 ppm (s, 3H); ^{13}C NMR (100 MHz, $[D_6]DMSO$): δ = 165.2, 164.8, 152.7, 140.6, 139.7, 139.0, 133.4, 132.4, 130.9, 130.4, 129.8, 129.3, 129.1, 128.9, 127.3, 124.2, 120.2, 120.1, 115.5, 56.6, 21.5 ppm; MS (ESI): m/z (%): 452 $[M+H]^+$ (100%), 474 $[M+Na]^+$ (20%); HRMS (MALDI): m/z calcd for $C_{27}H_{22}N_3O_2S$ $[M+H]^+$: 452.1427, found: 452.1423; HPLC (method A): t_R = 21.30 min (96.5%).

(Z)-4-(7-Methyl-2-(3-nitrobenzylidene)-3-oxo-6-(phenylcarbamoyl)thiazolo[3,2-*a*]pyrimidin-5-yl)-1,2-phenylene diacetate (BCL-LZH-24): General procedure A afforded BCL-LZH-24 as a yellow solid (94 mg, 47%). R_f 0.30 (silica gel, CH_2Cl_2/THF 50:1); 1H NMR (300 MHz, $CDCl_3$): δ = 8.35 (s, 1H), 8.26 (dd, J = 8.1, 0.9 Hz, 1H), 7.79–7.76 (m, 2H), 7.67 (t, J = 7.8 Hz, 1H), 7.38–7.34 (m, 3H), 7.30–7.25 (m, 3H), 7.21 (s, 1H), 7.16 (d, J = 8.4 Hz, 1H), 7.09 (t, J = 7.2 Hz, 1H), 6.17 (s, 1H), 2.29 (s, 6H), 2.27 ppm (s, 3H); ^{13}C NMR (100 MHz, $CDCl_3$): δ = 168.4, 168.1, 165.0, 164.4, 152.5, 148.6, 142.6, 142.5, 141.1, 137.2, 137.0, 135.2, 134.9, 130.4, 129.9, 128.9, 126.3, 124.9, 124.4, 124.1, 124.0, 123.4, 122.8, 120.5, 115.1, 67.9, 55.8, 25.6, 21.3, 20.7, 20.6 ppm; MS (ESI): m/z (%): 613 $[M+H]^+$ (12%), 635 $[M+Na]^+$ (100%), 651 $[M+K]^+$ (27%); HRMS (MALDI): m/z calcd for $C_{31}H_{24}N_4O_8SNa$ $[M+Na]^+$: 635.1207, found: 635.1181; HPLC (method A): t_R = 12.45 min (90.6%).

(Z)-Ethyl 2-(4-ethylbenzylidene)-7-methyl-3-oxo-5-phenylthiazolo[3,2-*a*]pyrimidine-6-carboxylate (BCL-LZH-25): General procedure A afforded BCL-LZH-25 as a yellow solid (77 mg, 54%). 1H NMR (300 MHz, $CDCl_3$): δ = 7.72 (s, 1H), 7.45–7.23 (m, 9H), 6.20 (s, 1H), 4.10 (q, J = 7.2 Hz, 2H), 2.68 (q, J = 7.5 Hz, 2H), 2.52 (s, 3H), 1.31–1.16 ppm (m, 6H); ^{13}C NMR (100 MHz, $CDCl_3$): δ = 165.5, 165.3, 156.5, 152.5, 147.5, 140.1, 133.7, 130.7, 130.3, 128.8, 128.7, 128.6, 128.1, 119.0, 109.0, 60.5, 55.5, 28.9, 22.8, 15.2, 14.1 ppm; MS

(MALDI): m/z (%): 433 $[M+H]^+$ (100%), 455 $[M+Na]^+$ (13%); HRMS (MALDI): m/z calcd for $C_{25}H_{24}N_2O_3S$ $[M]^+$: 432.1502, found: 432.1508; HPLC (method A): t_R = 24.14 min (89.9%).

(Z)-Ethyl 2-(2,5-dimethoxybenzylidene)-5-(4-ethylphenyl)-7-methyl-3-oxo-thiazolo[3,2-*a*]pyrimidine-6-carboxylate (BCL-LZH-26): General procedure A afforded BCL-LZH-26 as a yellow solid (104 mg, 64%). 1H NMR (300 MHz, $CDCl_3$): δ = 8.06 (s, 1H), 7.31 (d, J = 8.4 Hz, 2H), 7.12 (d, J = 8.1 Hz, 2H), 6.95–6.91 (m, 2H), 6.84 (dd, J = 7.5, 1.4 Hz, 1H), 6.16 (s, 1H), 4.10 (q, J = 7.2 Hz, 2H), 3.80 (d, J = 6.6 Hz, 6H), 2.59 (d, J = 7.5 Hz, 2H), 2.51 (s, 3H), 1.22–1.16 ppm (m, 6H); ^{13}C NMR (100 MHz, $CDCl_3$): δ = 165.6, 165.3, 156.6, 153.5, 152.9, 152.2, 144.6, 137.5, 129.0, 128.0, 122.6, 120.4, 118.1, 113.6, 112.3, 109.0, 60.4, 55.9, 55.7, 55.2, 28.5, 22.8, 20.8, 15.3, 14.1 ppm; MS (ESI): m/z (%): 515 $[M+Na]^+$ (100%); HRMS (MALDI): m/z calcd for $C_{27}H_{29}N_2O_5S$ $[M+H]^+$: 493.1792, found: 493.1799; HPLC (method A): t_R = 24.28 min (66.5%).

(Z)-2-((1-(4-Ethylbenzyl)indol-3-yl)methylene)-7-methyl-3-oxo-*N*,5-diphenylthiazolo[3,2-*a*]pyrimidine-6-carboxamide (BCL-LZH-27): General procedure A afforded BCL-LZH-27 as a yellow solid (61 mg, 31%). 1H NMR (300 MHz, $CDCl_3$): δ = 9.05 (s, 0.2H), 8.05 (s, 0.8H), 7.73 (d, J = 7.2 Hz, 1H), 7.46 (d, J = 6.6 Hz, 2H), 7.39–7.00 (m, 17H), 6.17 (s, 1H), 5.32–5.29 (m, 2H), 2.68–2.58 (m, 2H), 2.33 (s, 3H), 1.26–1.16 ppm (m, 3H); ^{13}C NMR (100 MHz, $CDCl_3$): δ = 165.2, 144.5, 143.3, 139.5, 137.3, 136.5, 132.7, 130.2, 129.3, 129.2, 129.1, 129.0, 128.5, 128.3, 128.0, 127.5, 127.2, 126.7, 124.9, 124.6, 123.7, 121.8, 119.9, 118.9, 113.7, 113.4, 111.4, 110.5, 56.3, 50.7, 28.5, 21.7, 15.4 ppm; MS (ESI): m/z (%): 609 $[M+H]^+$ (100%), 631 $[M+Na]^+$ (10%); HRMS (MALDI): m/z calcd for $C_{38}H_{33}N_4O_2S$ $[M+H]^+$: 609.2319, found: 609.2327; HPLC (method A): t_R = 23.21 min (84.6%).

(Z)-4-(2-((1-(4-Ethylbenzyl)indol-3-yl)methylene)-7-methyl-3-oxo-6-(phenylcarbamoyl)thiazolo[3,2-*a*]pyrimidin-5-yl)phenyl acetate (BCL-LZH-28): General procedure A afforded BCL-LZH-28 as a yellow solid (63 mg, 29%). 1H NMR (300 MHz, $CDCl_3$): δ = 8.10 (s, 1H), 7.79 (dd, J = 7.5, 1.5 Hz, 1H), 7.46 (d, J = 7.5 Hz, 1H), 7.41 (s, 1H), 7.37–7.34 (m, 3H), 7.31–7.23 (m, 4H), 7.18 (d, J = 8.4 Hz, 2H), 7.11–7.08 (m, 5H), 6.99 (s, 1H), 6.20 (s, 1H), 5.35 (s, 2H), 2.64 (q, J = 7.5 Hz, 2H), 2.32 (s, 3H), 2.27 (s, 3H), 1.22 ppm (t, J = 7.8 Hz, 3H); ^{13}C NMR (100 MHz, $CDCl_3$): δ = 169.2, 165.2, 154.9, 151.1, 144.6, 143.2, 137.4, 137.1, 136.7, 132.8, 130.4, 129.1, 128.7, 128.1, 127.3, 125.3, 124.8, 123.8, 122.4, 121.9, 120.3, 119.1, 113.8, 113.4, 111.5, 110.6, 55.7, 50.8, 28.6, 21.8, 21.2, 15.5 ppm; MS (ESI): m/z (%): 667 $[M+H]^+$ (75%), 689 $[M+Na]^+$ (100%), 705 $[M+K]^+$ (28%); HRMS (MALDI): m/z calcd for $C_{40}H_{35}N_4O_4S$ $[M+H]^+$: 667.2374, found: 663.2378; HPLC (method B): t_R = 13.77 min (95.1%).

(Z)-4-(2-((1-(4-Ethylbenzyl)indol-3-yl)methylene)-7-methyl-3-oxo-6-(phenylcarbamoyl)thiazolo[3,2-*a*]pyrimidine-5-yl)-1,2-phenylene diacetate (BCL-LZH-29): General procedure A afforded BCL-LZH-29 as a yellow solid (95 mg, 40%). 1H NMR (300 MHz, $CDCl_3$): δ = 9.03 (s, 0.2H), 8.06 (s, 0.8H), 7.75–7.66 (m, 1H), 7.39–6.98 (m, 17H), 6.17 (s, 1H), 5.31 (s, 1.6H), 5.22 (d, J = 2.4 Hz, 0.4H), 2.62 (q, J = 7.5 Hz, 2H), 2.27 (s, 3H), 2.25 (s, 6H), 1.21 ppm (t, J = 7.8 Hz, 3H); ^{13}C NMR (100 MHz, $CDCl_3$): δ = 168.5, 168.1, 165.6, 165.3, 154.6, 144.7, 142.7, 142.3, 138.1, 137.6, 136.8, 133.0, 130.6, 129.2, 128.8, 128.6, 128.3, 127.5, 127.0, 126.5, 125.4, 124.9, 124.2, 124.0, 123.1, 122.0, 120.6, 119.3, 114.2, 113.5, 111.7, 110.8, 55.6, 51.0, 30.6, 28.7, 21.8, 21.7, 21.0, 20.9, 15.7 ppm; MS (ESI): m/z (%): 725 $[M+H]^+$ (55%), 747 $[M+Na]^+$ (100%), 763 $[M+K]^+$ (15%); HRMS (MALDI): m/z calcd for $C_{42}H_{37}N_4O_6S$ $[M+H]^+$: 725.2428, found: 725.2425; HPLC (method B): t_R = 13.41 min (98.3%).

(Z)-Ethyl 2-((1-(4-ethylbenzyl)indol-3-yl)methylene)-7-methyl-3-oxo-5-phenylthiazolo[3,2-*a*]pyrimidine-6-carboxylate (BCL-LZH-30): General procedure A afforded BCL-LZH-30 as a yellow solid (72 mg, 39%). 1H NMR (300 MHz, $CDCl_3$): δ = 8.08 (s, 1H), 7.78–7.64 (m, 1H), 7.45–6.70 (m, 13H), 6.20–6.18 (m, 0.8H), 5.89–5.88 (m, 0.2H), 5.41–5.30 (m, 2H), 4.15–3.98 (m, 2H), 2.64 (q, J = 7.8 Hz, 2H), 2.53 (s, 2.4H), 2.34 (s, 0.6H), 1.25–1.10 ppm (m, 6H); ^{13}C NMR (100 MHz, $CDCl_3$): δ = 165.6, 165.2, 156.6, 152.8, 144.5, 140.4, 136.5, 132.6, 130.2, 128.5, 128.3, 128.2, 128.1, 127.9, 127.8, 127.2, 126.7, 126.5, 125.2, 123.7, 121.8, 118.9, 113.7, 111.4, 110.5, 108.4, 60.3, 55.3, 50.7, 28.5, 22.8, 15.4, 14.0 ppm; MS (ESI): m/z (%): 562 $[M+H]^+$ (100%), 584 $[M+Na]^+$ (5%), 600 $[M+K]^+$ (1%); HRMS (MALDI): m/z calcd for $C_{34}H_{32}N_3O_3S$ $[M+H]^+$: 562.2159, found: 562.2154; HPLC (method A): t_R = 25.17 min (61.5%).

(Z)-Methyl 5-(4-acetoxypheyl)-2-((1-(4-ethylbenzyl)indol-3-yl)methylene)-7-methyl-3-oxothiazolo[3,2-*a*]pyrimidine-6-carboxylate (BCL-LZH-31): General procedure A afforded BCL-LZH-31 as a yellow solid (63 mg, 32%). 1H NMR (300 MHz, $CDCl_3$): δ = 8.10 (s, 1H), 7.79–7.70 (m, 1H), 7.47–6.91 (m, 12H), 6.22–6.20 (m, 0.8H), 5.90–5.89 (m, 0.2H), 5.36–5.31 (m, 2H), 3.67–3.57 (m, 3H), 2.67–2.59 (m, 2H), 2.52–2.50 (m, 2.4H), 2.32–2.31 (m, 0.6H), 2.29–2.27 (m, 3H), 1.26–1.16 ppm (m, 3H); ^{13}C NMR (100 MHz, $CDCl_3$): δ = 169.2, 166.0, 165.2, 156.8, 153.5, 150.6, 144.5, 137.8, 136.5, 132.6, 130.3, 129.1, 129.0, 128.5, 128.3, 128.0, 127.2, 126.7, 126.4, 125.5, 123.7, 121.8, 121.6, 118.9, 113.6, 111.4, 110.5, 107.9, 54.4, 51.5, 50.7, 28.5, 22.9, 21.1, 15.4 ppm; MS (ESI): m/z (%): 606 $[M+H]^+$ (100%), 628 $[M+Na]^+$ (28%); HRMS (MALDI): m/z calcd for $C_{35}H_{32}N_3O_5S$ $[M+H]^+$: 606.2057, found: 606.2061; HPLC (method A): t_R = 23.84 min (81.6%).

(Z)-2-((1-(Biphenyl-4-ylmethyl)indol-3-yl)methylene)-7-methyl-3-oxo-*N*,5-diphenylthiazolo[3,2-*a*]pyrimidine-6-carboxamide (BCL-LZH-32): General procedure A afforded BCL-LZH-32 as a yellow solid (133 mg, 61%). 1H NMR (300 MHz, $CDCl_3$): δ = 8.10 (s, 1H), 7.78 (d, J = 7.2 Hz, 1H), 7.56 (d, J = 8.4 Hz, 4H), 7.48–7.22 (m, 18H), 7.09 (t, J = 6.9 Hz, 1H), 6.98 (s, 1H), 6.17 (s, 1H), 5.43 (s, 2H), 2.33 ppm (s, 3H); ^{13}C NMR (100 MHz, $CDCl_3$): δ = 165.1, 154.6, 143.3, 141.2, 140.2, 139.5, 137.3, 136.5, 134.5, 130.2, 129.3, 129.1, 129.0, 128.8, 128.0, 127.7, 127.5, 127.4, 127.0, 124.8, 124.6, 123.8, 121.8, 119.9, 119.0, 113.8, 113.7, 111.6, 110.5, 56.3, 50.7, 21.7 ppm; MS (ESI): m/z (%): 657 $[M+H]^+$ (100%), 679 $[M+Na]^+$ (48%); HRMS (ESI): m/z calcd for $C_{42}H_{32}N_4NaO_2S$ $[M+Na]^+$: 679.2138, found: 679.2144; HPLC (method A): t_R = 23.47 min (91.6%).

(Z)-2-((1-(Biphenyl-4-ylmethyl)indol-3-yl)methylene)-5-(4-fluorophenyl)-7-methyl-3-oxo-*N*-phenylthiazolo[3,2-*a*]pyrimidine-6-carboxamide (BCL-LZH-33): General procedure A afforded BCL-LZH-33 as a yellow solid (71 mg, 32%). 1H NMR (300 MHz, $CDCl_3$): δ = 8.10 (s, 1H), 7.79 (d, J = 7.2 Hz, 1H), 7.56 (d, J = 8.1 Hz, 4H), 7.46–7.42 (m, 5H), 7.37–7.22 (m, 10H), 7.13–7.02 (m, 4H), 6.19 (s, 1H), 5.43 (s, 2H), 2.33 ppm (s, 3H); ^{13}C NMR (100 MHz, $[D_6]DMSO$): δ = 164.9, 164.4, 152.8, 140.9, 139.6, 138.6, 136.2, 136.0, 131.7, 129.3, 129.2, 128.9, 128.6, 127.8, 127.5, 127.0, 126.6, 124.0, 123.7, 123.4, 121.5, 119.7, 118.8, 115.7, 115.5, 114.3, 112.8, 111.3, 110.2, 55.4, 49.5, 21.3 ppm; MS (ESI): m/z (%): 675 $[M+H]^+$ (100%), 697 $[M+Na]^+$ (11%); HRMS (MALDI): m/z calcd for $C_{42}H_{32}FN_4O_2S$ $[M+H]^+$: 675.2225, found: 675.2220; HPLC (method A): t_R = 23.63 min (93.9%).

(Z)-2-((1-(Biphenyl-4-ylmethyl)indol-3-yl)methylene)-5-(3-chlorophenyl)-7-methyl-3-oxo-*N*-phenylthiazolo[3,2-*a*]pyrimidine-6-carboxamide (BCL-LZH-34): General procedure A afforded BCL-LZH-34 as a yellow solid (125 mg, 55%). 1H NMR (300 MHz, $CDCl_3$): δ = 8.11 (s, 1H), 7.80 (dd, J = 7.2, 2.1 Hz, 1H), 7.57 (d, J = 8.4 Hz, 4H),

7.48–7.21 (m, 17H), 7.11 (t, $J=7.2$ Hz, 1H), 7.04 (s, 1H), 6.19 (s, 1H), 5.44 (s, 2H), 2.32 ppm (s, 3H); ^{13}C NMR (100 MHz, $[\text{D}_6]\text{DMSO}$): $\delta=164.8, 164.4, 152.9, 141.9, 141.2, 139.6, 138.5, 136.2, 136.0, 133.3, 131.8, 130.8, 128.9, 128.7, 128.5, 127.8, 127.5, 127.0, 126.8, 126.6, 125.8, 124.2, 123.8, 121.5, 119.8, 118.9, 113.8, 112.6, 111.3, 110.2, 55.6, 49.5, 21.3$ ppm; MS (MALDI): m/z (%): 691 $[\text{M}+\text{H}]^+$ (100%), 713 $[\text{M}+\text{Na}]^+$ (14%), 729 $[\text{M}+\text{K}]^+$ (6%); HRMS (MALDI): m/z calcd for $\text{C}_{42}\text{H}_{32}\text{ClN}_4\text{O}_2\text{S}$ $[\text{M}+\text{H}]^+$: 691.1929, found: 691.1937; HPLC (method B): $t_R=14.72$ min (80.2%).

(Z)-2-((1-(Biphenyl-4-ylmethyl)indol-3-yl)methylene)-5-(4-bromophenyl)-7-methyl-3-oxo-*N*-phenyl-thiazolo[3,2-*a*]pyrimidine-6-carboxamide (BCL-LZH-35): General procedure A afforded BCL-LZH-35 as a yellow solid (71 mg, 29%). ^1H NMR (300 MHz, $[\text{D}_6]\text{DMSO}$): $\delta=10.05$ (s, 1H), 8.18 (s, 1H), 8.05 (s, 1H), 7.91 (d, $J=7.8$ Hz, 1H), 7.64–7.55 (m, 9H), 7.46–7.18 (m, 11H), 7.06 (t, $J=7.5$ Hz, 1H), 6.22 (s, 1H), 5.66 (s, 2H), 2.13–2.08 ppm (m, 3H); ^{13}C NMR (100 MHz, $[\text{D}_6]\text{DMSO}$): $\delta=165.3, 164.8, 153.3, 141.4, 140.0, 139.5, 139.0, 136.7, 132.2, 129.6, 129.3, 129.1, 128.2, 127.9, 127.4, 127.0, 123.8, 122.0, 120.2, 119.2, 114.4, 113.1, 110.6, 56.0, 49.9, 21.7$ ppm; MS (MALDI): m/z (%): 735 $[\text{M}+\text{H}]^+$ (100%); HRMS (MALDI): m/z calcd for $\text{C}_{42}\text{H}_{32}\text{BrN}_4\text{O}_2\text{S}$ $[\text{M}+\text{H}]^+$: 735.1424, found: 735.1417; HPLC (method A): $t_R=15.04$ min (90.0%).

(Z)-2-((1-(Biphenyl-4-ylmethyl)indol-3-yl)methylene)-5-(4-ethylphenyl)-7-methyl-3-oxo-*N*-phenyl-thiazolo[3,2-*a*]pyrimidine-6-carboxamide (BCL-LZH-36): General procedure A afforded BCL-LZH-36 as a yellow solid (115 mg, 51%). ^1H NMR (300 MHz, CDCl_3): $\delta=8.10$ (s, 1H), 7.78 (d, $J=6.9$ Hz, 1H), 7.56 (d, $J=7.8$ Hz, 4H), 7.46–7.17 (m, 17H), 7.08 (t, $J=6.3$ Hz, 1H), 6.97 (s, 1H), 6.13 (s, 1H), 5.43 (s, 2H), 2.62 (q, $J=7.5$ Hz, 2H), 2.33 (s, 3H), 1.20 ppm (t, $J=7.8$ Hz, 3H); ^{13}C NMR (100 MHz, $[\text{D}_6]\text{DMSO}$): $\delta=165.1, 164.4, 152.8, 143.9, 140.8, 139.6, 138.7, 137.2, 136.2, 136.0, 131.6, 128.9, 128.6, 128.2, 127.8, 127.0, 126.8, 126.6, 123.9, 123.6, 123.4, 121.5, 119.7, 118.8, 114.6, 113.0, 111.3, 110.2, 55.7, 49.4, 27.8, 21.2, 21.0, 15.3$ ppm; MS (MALDI): m/z (%): 685 $[\text{M}+\text{H}]^+$ (100%), 707 $[\text{M}+\text{Na}]^+$ (12%); HRMS (MALDI): m/z calcd for $\text{C}_{44}\text{H}_{37}\text{N}_4\text{O}_2\text{S}$ $[\text{M}+\text{H}]^+$: 685.2632, found: 685.2623; HPLC (method A): $t_R=14.85$ min (75.4%).

(Z)-3-2-((1-(Biphenyl-4-ylmethyl)indol-3-yl)methylene)-7-methyl-3-oxo-6-(phenylcarbamoyl)thiazolo[3,2-*a*]pyrimidin-5-yl)phenyl acetate (BCL-LZH-37): General procedure A afforded BCL-LZH-37 as a yellow solid (109 mg, 46%). ^1H NMR (300 MHz, CDCl_3): $\delta=8.11$ (s, 1H), 7.80 (dd, $J=7.2, 1.5$ Hz, 1H), 7.56 (d, $J=8.4$ Hz, 4H), 7.47–7.41 (m, 3H), 7.38–7.33 (m, 7H), 7.29–7.18 (m, 7H), 7.10–7.03 (m, 2H), 6.18 (s, 1H), 5.44 (s, 2H), 2.29 ppm (s, 6H); ^{13}C NMR (100 MHz, CDCl_3): $\delta=169.5, 165.2, 151.3, 142.2, 141.3, 140.9, 140.4, 137.5, 136.6, 134.7, 130.4, 130.2, 129.0, 128.9, 128.1, 127.8, 127.7, 127.6, 127.2, 125.6, 125.0, 124.8, 123.9, 122.3, 122.0, 121.0, 120.3, 119.1, 114.2, 113.6, 111.7, 110.6, 56.0, 50.8, 21.5, 21.3$ ppm; MS (ESI): m/z (%): 715 $[\text{M}+\text{H}]^+$ (38%), 737 $[\text{M}+\text{Na}]^+$ (100%), 753 $[\text{M}+\text{K}]^+$ (11%); HRMS (MALDI): m/z calcd for $\text{C}_{44}\text{H}_{35}\text{N}_4\text{O}_4\text{S}$ $[\text{M}+\text{H}]^+$: 715.2374, found: 715.2369; HPLC (method B): $t_R=14.07$ min (81.9%).

(Z)-4-2-((1-(Biphenyl-4-ylmethyl)indol-3-yl)methylene)-7-methyl-3-oxo-6-(phenylcarbamoyl)thiazolo[3,2-*a*]pyrimidin-5-yl)phenyl acetate (BCL-LZH-38): General procedure A afforded BCL-LZH-38 as a yellow solid (87 mg, 37%). ^1H NMR (300 MHz, $[\text{D}_6]\text{DMSO}$): $\delta=10.05$ (s, 0.9H), 10.00 (s, 0.1H), 9.09 (s, 0.1H), 8.16 (s, 0.9H), 8.07 (s, 0.9H), 7.96 (s, 0.1H), 7.92 (d, $J=7.8$ Hz, 1H), 7.65–7.56 (m, 7H), 7.46–7.19 (m, 11H), 7.14–7.04 (m, 3H), 6.27 (s, 1H), 5.66 (s, 1.8H), 5.62 (s, 0.2H), 2.23 (s, 2.7H), 2.21 (s, 0.3H), 2.14 (s, 2.7H), 2.11 ppm (s, 0.3H); ^{13}C NMR (100 MHz, $[\text{D}_6]\text{DMSO}$): $\delta=169.0, 165.0, 164.4, 152.9, 150.3, 141.0, 139.6, 138.6, 137.2, 136.2, 136.0, 131.7, 128.9, 128.7, 128.0,$

127.8, 127.5, 127.0, 126.6, 124.1, 123.7, 122.2, 121.5, 119.8, 118.9, 114.3, 112.8, 111.3, 110.3, 55.4, 49.5, 30.4, 21.3, 20.8 ppm; MS (ESI): m/z (%): 715 $[\text{M}+\text{H}]^+$ (100%), 737 $[\text{M}+\text{Na}]^+$ (50%), 753 $[\text{M}+\text{K}]^+$ (19%); HRMS (MALDI): m/z calcd for $\text{C}_{44}\text{H}_{35}\text{N}_4\text{O}_4\text{S}$ $[\text{M}+\text{H}]^+$: 715.2374, found: 715.2369; HPLC (method A): $t_R=23.15$ min (94.0%).

(Z)-4-2-((1-(Biphenyl-4-ylmethyl)indol-3-yl)methylene)-7-methyl-3-oxo-6-(phenylcarbamoyl)thiazolo[3,2-*a*]pyrimidin-5-yl)-1,2-phenylene diacetate (BCL-LZH-39): General procedure A afforded BCL-LZH-39 as a yellow solid (63 mg, 25%). ^1H NMR (300 MHz, CDCl_3): $\delta=9.10$ (s, 0.1H), 8.11 (s, 0.9H), 7.80 (d, $J=7.8$ Hz, 1H), 7.57–7.06 (m, 22H), 6.18 (s, 1H), 5.43 (s, 1.8H), 5.37 (s, 0.2H), 2.27 ppm (s, 9H); ^{13}C NMR (100 MHz, $[\text{D}_6]\text{DMSO}$): $\delta=168.0, 167.9, 164.9, 164.4, 152.9, 142.1, 142.0, 141.4, 139.6, 138.6, 138.3, 136.2, 136.1, 131.8, 128.9, 128.6, 127.8, 127.5, 127.0, 126.6, 125.1, 124.3, 124.1, 123.7, 123.4, 121.9, 121.5, 120.0, 118.9, 113.8, 112.7, 111.3, 110.3, 55.1, 49.5, 21.3, 20.3$ ppm; MS (ESI): m/z (%): 773 $[\text{M}+\text{H}]^+$ (36%), 795 $[\text{M}+\text{Na}]^+$ (100%), 811 $[\text{M}+\text{K}]^+$ (20%); HRMS (MALDI): m/z calcd for $\text{C}_{46}\text{H}_{37}\text{N}_4\text{O}_6\text{S}$ $[\text{M}+\text{H}]^+$: 773.2428, found: 773.2435; HPLC (method B): $t_R=13.82$ min (94.3%).

(Z)-Ethyl 2-((1-(biphenyl-4-ylmethyl)indol-3-yl)methylene)-7-methyl-3-oxo-5-phenylthiazolo[3,2-*a*]pyrimidine-6-carboxylate (BCL-LZH-40): General procedure A afforded BCL-LZH-40 as a yellow solid (59 mg, 30%). ^1H NMR (300 MHz, CDCl_3): $\delta=8.08$ (s, 1H), 7.78–7.75 (m, 1H), 7.56–7.15 (m, 18H), 6.19–6.16 (m, 1H), 5.44–5.38 (m, 2H), 4.10 (q, $J=7.2$ Hz, 2H), 2.52 (s, 3H), 1.19 ppm (t, $J=7.2$ Hz, 3H); ^{13}C NMR (100 MHz, CDCl_3): $\delta=165.6, 165.2, 156.5, 152.7, 141.2, 140.4, 140.2, 136.5, 134.5, 130.2, 128.8, 128.7, 128.5, 127.9, 127.8, 127.7, 127.5, 127.4, 127.1, 127.0, 126.9, 125.1, 123.8, 121.8, 118.9, 114.0, 111.5, 110.5, 108.4, 60.3, 55.3, 50.6, 22.8, 14.0$ ppm; MS (ESI): m/z (%): 610 $[\text{M}+\text{H}]^+$ (100%), 632 $[\text{M}+\text{Na}]^+$ (5%); HRMS (MALDI): m/z calcd for $\text{C}_{38}\text{H}_{32}\text{N}_3\text{O}_3\text{S}$ $[\text{M}+\text{H}]^+$: 610.2159, found: 610.2161; HPLC (method A): $t_R=25.48$ min (80.5%).

(Z)-Ethyl 2-((1-(biphenyl-4-ylmethyl)indol-3-yl)methylene)-5-(4-fluorophenyl)-7-methyl-3-oxo-thiazolo[3,2-*a*]pyrimidine-6-carboxylate (BCL-LZH-41): General procedure A afforded BCL-LZH-41 as a yellow solid (141 mg, 68%). ^1H NMR (300 MHz, CDCl_3): $\delta=8.12$ (s, 0.8H), 7.80 (dd, $J=7.5, 1.8$ Hz, 0.8H), 7.67 (s, 0.2H), 7.56 (d, $J=8.1$ Hz, 4H), 7.46–7.19 (m, 10H), 7.01–6.91 (m, 2.6H), 6.68 (t, $J=8.4$ Hz, 0.4H), 6.20 (s, 0.8H), 5.84 (s, 0.2H), 5.45–5.43 (m, 2H), 5.19 (s, 0.2H), 4.11 (q, $J=6.6$ Hz, 1.6H), 4.02–3.97 (m, 0.4H), 2.52 (s, 2.4H), 2.31 (s, 0.6H), 1.19 (d, $J=7.5$ Hz, 2.4H), 1.09 ppm (d, $J=7.2$ Hz, 0.6H); ^{13}C NMR (100 MHz, CDCl_3): $\delta=165.5, 165.1, 156.4, 152.9, 141.2, 140.1, 136.5, 134.5, 130.3, 130.0, 129.9, 128.8, 127.9, 127.7, 127.6, 127.5, 127.0, 125.2, 123.9, 121.9, 118.9, 115.5, 115.3, 113.7, 111.5, 110.5, 108.3, 60.4, 54.6, 50.6, 22.9, 14.1$ ppm; MS (ESI): m/z (%): 628 $[\text{M}+\text{H}]^+$ (100%), 650 $[\text{M}+\text{Na}]^+$ (10%); HRMS (ESI): m/z calcd for $\text{C}_{38}\text{H}_{31}\text{FN}_3\text{O}_3\text{S}$ $[\text{M}+\text{H}]^+$: 628.2065, found: 628.2076; HPLC (method B): $t_R=16.14$ min (60.0%).

(Z)-Ethyl 2-((1-(biphenyl-4-ylmethyl)indol-3-yl)methylene)-5-(3-methoxyphenyl)-7-methyl-3-oxo-thiazolo[3,2-*a*]pyrimidine-6-carboxylate (BCL-LZH-42): General procedure A afforded BCL-LZH-42 as a yellow solid (131 mg, 62%). ^1H NMR (300 MHz, CDCl_3): $\delta=8.09$ (s, 1H), 7.79–7.76 (m, 0.8H), 7.72–7.68 (m, 0.2H), 7.56–7.53 (m, 4H), 7.45–7.06 (m, 8H), 7.03–6.94 (m, 2H), 7.79 (d, $J=7.8$ Hz, 1H), 6.67–6.49 (m, 1H), 6.17 (s, 0.8H), 5.89 (s, 0.2H), 4.12 (q, $J=7.2$ Hz, 1.6H), 4.01 (q, $J=7.2$ Hz, 0.4H), 3.76–3.74 (m, 2.4H), 3.50–3.48 (m, 0.6H), 2.46 (s, 2.4H), 3.30 (s, 0.6H), 1.21 (t, $J=7.2$ Hz, 2.4H), 1.12 ppm (t, $J=6.9$ Hz, 0.6H); ^{13}C NMR (100 MHz, CDCl_3): $\delta=165.6, 165.2, 159.6, 156.4, 152.8, 141.9, 141.2, 140.6, 140.2, 136.5, 134.5, 130.2, 129.5, 128.8, 128.0, 127.7, 127.5, 127.4, 127.0, 126.9, 125.0, 123.8, 121.8,$

120.2, 119.0, 114.0, 113.8, 113.7, 111.5, 110.5, 108.4, 60.4, 55.2, 55.1, 50.6, 22.8, 14.1 ppm; MS (ESI): m/z (%): 640 $[M+H]^+$ (100%), 662 $[M+Na]^+$ (8%), 678 $[M+K]^+$ (4%); HRMS (MALDI): m/z calcd for $C_{39}H_{34}N_3O_4S$ $[M+H]^+$: 640.2265, found: 640.2266; HPLC (method B): t_R = 16.44 min (75.9%).

(Z)-Methyl 5-(4-acetoxyphe-nyl)-2-((1-(biphenyl-4-ylmethyl)indol-3-yl)methylene)-7-methyl-3-oxothiazolo[3,2-*a*]pyrimidine-6-carboxylate (BCL-LZH-43): General procedure A afforded BCL-LZH-43 as a yellow solid (48 mg, 22%). 1H NMR (300 MHz, $CDCl_3$): δ = 8.12 (s, 1H), 7.82–7.79 (m, 1H), 7.57–6.74 (m, 17H), 6.23–6.20 (m, 1H), 5.44–5.43 (m, 2H), 3.67–3.53 (m, 3H), 2.52–2.50 (m, 2.5H), 2.30–2.23 ppm (m, 3.5H); ^{13}C NMR (100 MHz, $CDCl_3$): δ = 169.2, 166.0, 165.2, 156.7, 153.5, 150.6, 141.2, 140.2, 137.8, 136.5, 134.5, 130.3, 129.1, 129.0, 128.8, 128.0, 127.7, 127.6, 127.5, 127.4, 127.1, 127.0, 125.4, 123.8, 121.9, 121.7, 121.6, 119.0, 117.9, 113.9, 111.6, 110.5, 107.9, 54.4, 51.5, 50.7, 22.9, 21.1 ppm; MS (ESI): m/z (%): 654 $[M+H]^+$ (100%), 676 $[M+Na]^+$ (35%), 692 $[M+K]^+$ (14%); HRMS (MALDI): m/z calcd for $C_{39}H_{32}N_3O_5S$ $[M+H]^+$: 654.2057, found: 654.2070; HPLC (method A): t_R = 25.67 min (60.4%).

Preparation of Biginelli products 3 (general procedure B): β -Keto ester or amide **1** (10 mmol) and substituted aldehyde **2** (10 mmol) were added to a stirred solution of thiourea (762 mg, 10 mmol) in EtOH (25 mL) at RT. *p*-TsOH·H₂O (190 mg, 1 mmol) was added to the solution. The mixture was brought to reflux for 24 h and then cooled to RT. The crude reaction mixture was filtered, washed several times with petroleum ether and dried in vacuo to afford the Biginelli products **3a–3t**.

6-Methyl-*N*,4-diphenyl-2-thioxo-1,2,3,4-tetrahydropyrimidine-5-carboxamide (3a): General procedure B afforded **3a** as a white solid (2.005 g, 62%). 1H NMR (300 MHz, $[D_6]DMSO$): δ = 10.00 (s, 1H), 9.74 (s, 1H), 9.45 (s, 1H), 7.54 (d, J = 8.1 Hz, 2H), 7.38–7.33 (m, 2H), 7.29–7.23 (m, 5H), 7.02 (d, J = 7.5 Hz, 1H), 5.40 (d, J = 2.4 Hz, 1H), 2.07 ppm (s, 3H).

4-(4-Fluorophenyl)-6-methyl-*N*-phenyl-2-thioxo-1,2,3,4-tetrahydropyrimidine-5-carboxamide (3b): General procedure B afforded **3b** as a white solid (2.253 g, 66%). 1H NMR (300 MHz, $[D_6]DMSO$): δ = 10.04 (s, 1H), 9.74 (s, 1H), 9.46 (s, 1H), 7.54 (d, J = 7.8 Hz, 2H), 7.31–7.17 (m, 6H), 7.02 (t, J = 7.2 Hz, 1H), 5.39 (d, J = 3.0 Hz, 1H), 2.07 ppm (s, 3H).

4-(3-Chlorophenyl)-6-methyl-*N*-phenyl-2-thioxo-1,2,3,4-tetrahydropyrimidine-5-carboxamide (3c): General procedure B afforded **3c** as a white solid (2.326 g, 65%). 1H NMR (300 MHz, $[D_6]DMSO$): δ = 10.10 (s, 1H), 9.77 (s, 1H), 9.49 (s, 1H), 7.54 (d, J = 7.8 Hz, 2H), 7.43–7.33 (m, 2H), 7.29–7.20 (m, 4H), 7.03 (t, J = 7.5 Hz, 1H), 5.39 (d, J = 3.0 Hz, 1H), 2.08 ppm (s, 3H); MS (EI): m/z (%): 357 $[M]^+$ (29), 93 (100).

4-(4-Bromophenyl)-6-methyl-*N*-phenyl-2-thioxo-1,2,3,4-tetrahydropyrimidine-5-carboxamide (3d): General procedure B afforded **3d** as a white solid (1.006 g, 25%). 1H NMR (300 MHz, $[D_6]DMSO$): δ = 10.07 (s, 1H), 9.74 (s, 1H), 9.47 (s, 1H), 7.55 (td, J = 9.0, 1.2 Hz, 4H), 7.26 (t, J = 7.8 Hz, 2H), 7.20 (d, J = 8.4 Hz, 2H), 7.02 (t, J = 7.2 Hz, 1H), 5.37 (d, J = 3.0 Hz, 1H), 2.06 ppm (s, 3H).

4-(4-Methoxyphenyl)-6-methyl-*N*-phenyl-2-thioxo-1,2,3,4-tetrahydropyrimidine-5-carboxamide (3e): General procedure B afforded **3e** as a white solid (3.534 g, 100%). 1H NMR (300 MHz, $[D_6]DMSO$): δ = 10.07 (s, 0.2H), 9.95 (s, 0.8H), 9.80 (s, 0.2H), 9.69 (s, 0.8H), 9.56 (s, 0.2H), 9.39 (s, 0.8H), 7.54 (d, J = 7.5 Hz, 2H), 7.25 (t, J = 8.1 Hz, 2H), 7.18 (d, J = 9.0 Hz, 2H), 7.01 (t, J = 7.5 Hz, 1H), 6.91 (d, J = 8.7 Hz, 2H), 5.40 (d, J = 3.0 Hz, 0.2H), 5.35 (d, J = 2.7 Hz, 0.8H),

3.75 (s, 0.6H), 3.71 (s, 3H), 2.07 ppm (s, 2.4H); MS (ESI): m/z (%): 354 $[M+H]^+$ (100%), 376 $[M+Na]^+$ (37%).

4-(4-Ethylphenyl)-6-methyl-*N*-phenyl-2-thioxo-1,2,3,4-tetrahydropyrimidine-5-carboxamide (3f): General procedure B afforded **3f** as a white solid (1.968 g, 56%). 1H NMR (300 MHz, $[D_6]DMSO$): δ = 9.97 (s, 1H), 9.72 (s, 1H), 9.41 (s, 1H), 7.55 (d, J = 7.5 Hz, 2H), 7.25 (t, J = 8.1 Hz, 2H), 7.20–7.14 (m, 4H), 7.01 (t, J = 7.5 Hz, 1H), 5.37 (d, J = 2.7 Hz, 1H), 2.55 (q, J = 7.8 Hz, 2H), 2.06 (s, 3H), 1.14 ppm (t, J = 7.5 Hz, 3H); MS (EI): m/z (%): 351 $[M]^+$ (45), 259 (100); HRMS (EI): m/z calcd for $C_{26}H_{21}N_3OS$ $[M]^+$: 351.1405, found: 351.1408.

4-(3-Hydroxyphenyl)-6-methyl-*N*-phenyl-2-thioxo-1,2,3,4-tetrahydropyrimidine-5-carboxamide (3g): General procedure B afforded **3g** as a white solid (1.595 g, 47%). 1H NMR (300 MHz, $[D_6]DMSO$): δ = 9.96 (s, 1H), 9.72 (s, 1H), 9.46 (s, 1H), 9.39 (s, 1H), 7.56 (d, J = 7.8 Hz, 2H), 7.26 (t, J = 8.1 Hz, 2H), 7.11 (t, J = 8.1 Hz, 1H), 7.02 (t, J = 7.5 Hz, 1H), 6.66–6.63 (m, 3H), 5.32 (d, J = 3.0 Hz, 1H), 2.05 ppm (s, 3H); MS (EI): m/z (%): 339 $[M]^+$ (15), 247 (100).

4-(4-Hydroxyphenyl)-6-methyl-*N*-phenyl-2-thioxo-1,2,3,4-tetrahydropyrimidine-5-carboxamide (3h): General procedure B afforded **3h** as a white solid (1.324 g, 39%). 1H NMR (300 MHz, $[D_6]DMSO$): δ = 9.91 (s, 1H), 9.66 (s, 1H), 9.41 (s, 1H), 9.34 (s, 1H), 7.53 (d, J = 7.5 Hz, 2H), 7.25 (t, J = 7.8 Hz, 2H), 7.06 (d, J = 9.0 Hz, 2H), 7.01 (t, J = 7.2 Hz, 1H), 6.71 (d, J = 8.4 Hz, 2H), 5.29 (d, J = 2.7 Hz, 1H), 2.05 ppm (s, 3H); MS (ESI): m/z (%): 340 $[M+H]^+$ (100%), 352 $[M+Na]^+$ (45%).

4-(3,4-Dihydroxyphenyl)-6-methyl-*N*-phenyl-2-thioxo-1,2,3,4-tetrahydropyrimidine-5-carboxamide (3i): General procedure B afforded **3i** as a white solid (1.777 g, 50%). 1H NMR (300 MHz, $[D_6]DMSO$): δ = 9.87 (s, 1H), 9.64 (s, 1H), 9.31 (s, 1H), 8.94 (s, 1H), 8.87 (s, 1H), 7.54 (d, J = 7.5 Hz, 2H), 7.25 (t, J = 7.8 Hz, 2H), 7.01 (t, J = 7.5 Hz, 1H), 6.67–6.64 (m, 2H), 6.50 (dd, J = 8.4, 2.1 Hz, 1H), 5.24 (d, J = 2.4 Hz, 1H), 2.04 ppm (s, 3H); ^{13}C NMR (100 MHz, CD_3OD): δ = 175.4, 167.9, 146.7, 146.5, 139.2, 135.6, 135.0, 129.7, 125.5, 121.8, 119.2, 116.4, 114.9, 109.9, 57.6, 16.7 ppm; MS (ESI): m/z (%): 356 $[M+H]^+$ (100%), 378 $[M+Na]^+$ (38%); HRMS (ESI): m/z calcd for $C_{18}H_{18}N_3O_3S$ $[M+H]^+$: 356.1069, found: 356.1069.

Ethyl 6-methyl-4-phenyl-2-thioxo-1,2,3,4-tetrahydropyrimidine-5-carboxylate (3j): General procedure B afforded **3j** as a white solid (1.382 g, 50%). 1H NMR (300 MHz, $CDCl_3$): δ = 8.11 (s, 1H), 7.47 (s, 1H), 7.32–7.27 (m, 5H), 5.39 (d, J = 3.0 Hz, 1H), 4.08 (qd, J = 7.2, 2.7 Hz, 2H), 2.36 (s, 3H), 1.16 ppm (t, J = 7.2 Hz, 3H).

Ethyl 4-(4-fluorophenyl)-6-methyl-2-thioxo-1,2,3,4-tetrahydropyrimidine-5-carboxylate (3k): General procedure B afforded **3k** as a white solid (1.060 g, 36%). 1H NMR (300 MHz, $CDCl_3$): δ = 8.12 (s, 1H), 7.57 (s, 1H), 7.26 (td, J = 6.3 Hz, 2.1, 2H), 7.01 (t, J = 8.7 Hz, 2H), 5.38 (d, J = 3.0 Hz, 1H), 4.14–4.06 (m, 2H), 2.37 (s, 3H), 1.17 ppm (t, J = 7.2 Hz, 3H).

Ethyl 4-(3-chlorophenyl)-6-methyl-2-thioxo-1,2,3,4-tetrahydropyrimidine-5-carboxylate (3l): General procedure B afforded **3l** as a white solid (0.901 g, 29%). 1H NMR (300 MHz, $CDCl_3$): δ = 8.01 (s, 1H), 7.48 (s, 1H), 7.27 (d, J = 3.3 Hz, 3H), 7.20–7.16 (m, 1H), 5.37 (d, J = 3.0 Hz, 1H), 4.16–4.05 (m, 2H), 2.37 (s, 3H), 1.19 ppm (t, J = 7.5 Hz, 3H).

Ethyl 4-(3-methoxyphenyl)-6-methyl-2-thioxo-1,2,3,4-tetrahydropyrimidine-5-carboxylate (3m): General procedure B afforded **3m** as a white solid (1.409 g, 46%). 1H NMR (300 MHz, $CDCl_3$): δ = 8.01 (s, 1H), 7.42 (s, 1H), 7.24 (t, J = 8.4 Hz, 1H), 6.87 (d, J = 8.1 Hz, 1H), 6.83–6.81 (m, 2H), 5.37 (d, J = 3.0 Hz, 1H), 4.09 (qd, J = 7.2, 1.8 Hz, 2H), 3.78 (s, 3H), 2.36 (s, 3H), 1.18 ppm (t, J = 7.2 Hz, 3H).

Ethyl 4-(4-ethylphenyl)-6-methyl-2-thioxo-1,2,3,4-tetrahydropyrimidine-5-carboxylate (3n): General procedure B afforded **3n** as a white solid (1.735 g, 57%). ¹H NMR (300 MHz, [D₆]DMSO): δ = 10.31 (s, 1H), 9.62 (d, *J* = 1.8 Hz, 1H), 7.15 (q, *J* = 9.0 Hz, 4H), 5.13 (d, *J* = 3.3 Hz, 1H), 4.01 (q, *J* = 7.2 Hz, 2H), 2.56 (q, *J* = 7.5 Hz, 2H), 2.28 (s, 3H), 1.15 (t, *J* = 7.5 Hz, 3H), 1.11 ppm (t, *J* = 7.2 Hz, 3H).

N,6-Dimethyl-N,4-diphenyl-2-thioxo-1,2,3,4-tetrahydropyrimidine-5-carboxamide (3o): General procedure B afforded **3o** as a white solid (1.249 g, 37%). ¹H NMR (300 MHz, CDCl₃): δ = 7.70 (s, 1H), 7.41–7.34 (m, 3H), 7.30–7.22 (m, 5H), 6.77 (d, *J* = 7.8 Hz, 2H), 6.71 (s, 1H), 4.93 (s, 1H), 3.15 (s, 3H), 1.86 ppm (s, 3H); MS (EI): *m/z* (%): 337 [M]⁺ (19), 107 (100); HRMS (EI): *m/z* calcd for C₁₉H₁₉N₃O₂S [M]⁺: 337.1249, found: 337.1251.

4-(4-Hydroxyphenyl)-N,6-dimethyl-N-phenyl-2-thioxo-1,2,3,4-tetrahydropyrimidine-5-carboxamide (3p): General procedure B afforded **3p** as a white solid (0.742 g, 21%). ¹H NMR (300 MHz, [D₆]DMSO): δ = 9.69 (s, 1H), 9.45 (s, 1H), 8.88 (s, 1H), 7.37–7.24 (m, 3H), 7.07 (d, *J* = 7.2 Hz, 2H), 6.92 (d, *J* = 8.7 Hz, 2H), 6.73 (d, *J* = 8.7 Hz, 2H), 4.54 (s, 1H), 3.10 (s, 3H), 1.76 ppm (s, 3H); MS (EI): *m/z* (%): 353 [M]⁺ (26), 107 (100); HRMS (EI): *m/z* calcd for C₁₉H₁₉N₃O₂S [M]⁺: 353.1198, found: 353.1190.

N,6-Dimethyl-4-phenyl-2-thioxo-1,2,3,4-tetrahydropyrimidine-5-carboxamide (3q): General procedure B afforded **3q** as a white solid (1.124 g, 43%). ¹H NMR (300 MHz, [D₆]DMSO): δ = 10.38–10.35 (m, 1H), 9.69 (d, *J* = 1.8 Hz, 1H), 7.37–7.21 (m, 5H), 5.19 (d, *J* = 3.6 Hz, 1H), 3.55 (s, 3H), 2.30 ppm (s, 3H); MS (EI): *m/z* (%): 262 [M]⁺ (62.52), 185 (100).

4-(4-Hydroxyphenyl)-N,6-dimethyl-2-thioxo-1,2,3,4-tetrahydropyrimidine-5-carboxamide (3r): General procedure B afforded **3r** as a white solid (0.998 g, 36%). ¹H NMR (300 MHz, [D₆]DMSO): δ = 10.03 (s, 1H), 9.59 (s, 1H), 9.44 (s, 1H), 7.00 (d, *J* = 8.4 Hz, 2H), 6.71 (d, *J* = 8.4 Hz, 2H), 5.06 (d, *J* = 3.6 Hz, 1H), 3.54 (s, 3H), 2.28 ppm (s, 3H); MS (EI): *m/z* (%): 278 [M]⁺ (100).

Methyl 6-methyl-4-phenyl-2-thioxo-1,2,3,4-tetrahydropyrimidine-5-carboxylate (3s): General procedure B afforded **3s** as a white solid (1.784 g, 68%). ¹H NMR (300 MHz, [D₆]DMSO): δ = 9.86 (s, 1H), 9.36 (s, 1H), 7.72 (d, *J* = 4.2 Hz, 1H), 7.37–7.19 (m, 5H), 5.25 (d, *J* = 3.0 Hz, 1H), 2.55 (d, *J* = 4.5 Hz, 3H), 2.03 ppm (s, 3H); MS (EI): *m/z* (%): 261 [M]⁺ (100).

Methyl 4-(4-hydroxyphenyl)-6-methyl-2-thioxo-1,2,3,4-tetrahydropyrimidine-5-carboxylate (3t): General procedure B afforded **3t** as a white solid (1.559 g, 56%). ¹H NMR (300 MHz, [D₆]DMSO): δ = 9.77 (s, 1H), 9.42 (s, 1H), 9.26 (s, 1H), 7.64 (d, *J* = 4.5 Hz, 1H), 7.00 (d, *J* = 8.4 Hz, 2H), 6.70 (d, *J* = 8.7 Hz, 2H), 5.12 (d, *J* = 3.0 Hz, 1H), 2.53–2.51 (m, 3H), 2.02 ppm (s, 3H); MS (EI): *m/z* (%): 277 [M]⁺ (100).

1-Methyl-indole-3-carbaldehyde (4a): 60% NaH (0.642 g, 16.05 mmol) was added in portions to a stirred solution of **8** (2.002 g, 13.78 mmol) in dry DMF (30 mL) at 0 °C. The mixture was maintained at 0 °C for 10 min and then CH₃I (1.00 mL, 16.06 mmol) was added at the same temperature. The mixture was warmed to RT and stirred for 1 h. Ice water was added to quench the reaction. Solvent was removed in vacuo. The residue was washed with water, and the aqueous phase was then extracted with EtOAc (3 × 100 mL). The combined organic phase was washed with brine, dried (Na₂SO₄), filtered, and evaporated. The crude reaction mixture was purified by flash chromatography (silica gel, eluent EtOAc/petroleum ether 3:1) to give **4a** (1.483 g, 9.32 mmol, 68%) as a gray solid. ¹H NMR (300 MHz, CDCl₃): δ = 9.99 (s, 1H), 8.32–8.29 (m, 1H), 7.67 (s, 1H), 7.37–7.31 (m, 3H), 3.87 ppm (s, 3H).

1-Benzyl-indole-3-carbaldehyde (4b): **4b** was obtained from **8** and **7b** following the procedure of **4a**. Yellow solid (2.432 g, 75%). ¹H NMR (300 MHz, CDCl₃): δ = 10.01 (s, 1H), 8.35–8.32 (m, 1H), 7.72 (s, 1H), 7.38–7.29 (m, 6H), 7.19 (dd, *J* = 7.5, 2.7 Hz, 2H), 5.37 ppm (s, 2H); MS (ESI): *m/z* (%): 236 [M+H]⁺ (95%), 258 [M+Na]⁺ (100%).

1-(4-Ethylbenzyl)indole-3-carbaldehyde (4c): **4c** was obtained from **8** and **7c** following the procedure of **4a**. White solid (3.012 g, 83%). ¹H NMR (300 MHz, CDCl₃): δ = 9.99 (s, 1H), 8.34–8.31 (m, 1H), 7.70 (s, 1H), 7.38–7.30 (m, 3H), 7.20–7.10 (m, 4H), 5.32 (s, 2H), 2.64 (q, *J* = 7.5 Hz, 2H), 1.22 ppm (t, *J* = 7.5 Hz, 3H); ¹³C NMR (100 MHz, CDCl₃): δ = 184.6, 147.7, 144.5, 138.5, 137.4, 132.4, 128.5, 127.3, 125.4, 124.0, 122.9, 122.0, 118.3, 110.3, 50.6, 28.4, 15.4 ppm; MS (EI): *m/z* (%): 263 [M]⁺ (32), 119 (100); HRMS (EI): *m/z* calcd for C₁₈H₁₇NO [M]⁺: 263.1310, found: 263.1308.

1-(Biphenyl-4-ylmethyl)indole-3-carbaldehyde (4d): **4d** was obtained from **8** and **7d** following the procedure of **4a**. White solid (3.561 g, 87%). ¹H NMR (300 MHz, CDCl₃): δ = 10.01 (s, 1H), 8.34 (dd, *J* = 7.5, 2.7 Hz, 1H), 7.45 (s, 1H), 7.58–7.54 (m, 4H), 7.46–7.31 (m, 6H), 7.26–7.23 (m, 2H), 5.39 ppm (s, 2H); ¹³C NMR (100 MHz, CDCl₃): δ = 184.6, 141.3, 140.1, 138.5, 137.4, 134.2, 128.8, 127.7, 127.6, 127.0, 125.4, 124.1, 123.0, 122.1, 118.4, 110.4, 50.5 ppm; MS (EI): *m/z* (%): 311 [M]⁺ (25.33), 167 (100); HRMS (EI): *m/z* calcd for C₂₂H₁₇NO [M]⁺: 311.1310, found: 311.1309.

(4-Ethylphenyl)methanol (6c): NaBH₄ (1.702 g, 45 mmol) was added in portions to a stirred solution of 4-ethylbenzaldehyde **5c** (4.19 mL, 30 mmol) in MeOH (40 mL) at 0 °C. The mixture was stirring for 15 min. 1M HCl was added to quench the reaction. Solvent was removed in vacuo. The residue was diluted with CH₂Cl₂, washed with water, and extracted with CH₂Cl₂ (3 × 100 mL). The combined organic phase was washed with brine, dried (Na₂SO₄), filtered, and evaporated to give **6c** (4.061 g, 29.82 mmol, 99%) as a colorless oil.

1-(Bromomethyl)-4-ethylbenzene (7c): Tribromophosphine (3.00 mL, 31.61 mmol) was added dropwise to a stirred solution of **6c** (4.061 g, 29.82 mmol) in freshly distilled CH₂Cl₂ (100 mL) at 0 °C. The mixture was stirring for 6 h. Ice water was added to quench the reaction. Solvent was removed in vacuo. The residue was washed with water, and extracted with EtOAc (3 × 30 mL). The combined organic phase was washed with saturated NaHCO₃ solution, water and brine, dried (Na₂SO₄), filtered, and evaporated to give **7c** (5.867 g, 29.47 mmol, 98%) as a colorless oil. ¹H NMR (300 MHz, CDCl₃): δ = 7.31 (d, *J* = 7.8 Hz, 2H), 7.18 (d, *J* = 7.8 Hz, 2H), 4.50 (s, 2H), 2.65 (q, *J* = 7.5 Hz, 2H), 1.23 ppm (t, *J* = 7.8 Hz, 3H).

4-(Bromomethyl)biphenyl (7d): **7d** was obtained from biphenyl-4-ylmethanol **6d** following the procedure of **7c**. White solid (6.043 g, 82%). ¹H NMR (300 MHz, CDCl₃): δ = 7.60–7.57 (m, 4H), 7.49–7.34 (m, 5H), 4.56 ppm (s, 2H).

Indole-3-carbaldehyde (8): POCl₃ (10.00 mL, 0.11 mol) was added dropwise to a stirred solution of dry DMF (30 mL, 0.43 mol) at 0 °C. The mixture stirred at 0 °C for 30 min and then 1H-indole (11.715 g, 0.10 mol) in DMF (9.00 mL, 0.12 mol) was added dropwise at the same temperature. The mixture stirred at 0 °C for another 30 min and then warmed to RT and stirred for 3 h. Ice water (30 mL) was added carefully to quench the reaction. NaOH (19.200 g, 0.48 mol) in water (100 mL) was added in portions to quench the acid solution. The reaction mixture was brought to reflux for 1 h and then cooled to RT. The crude reaction mixture was filtered, and washed by water (5 × 50 mL), and dried in vacuo to give **8** (13.824 g, 95 mmol, 95%) as yellow crystals. ¹H NMR (300 MHz, CDCl₃): δ =

10.08 (s, 1H), 8.80 (br s, 1H), 8.34–8.31 (m, 1H), 7.86 (d, $J=3.3$ Hz, 1H), 7.46–7.43 (m, 1H), 7.35–7.32 ppm (m, 2H).

Biology

Protein expression and purification

Three Bcl-2 family proteins, that is, Bcl- x_L , Bcl-2, and Mcl-1, were used as target proteins in our *in vitro* binding assay. They were expressed and purified using the following methods.

Bcl- x_L : The plasmid of GST-Bcl- x_L protein built on the pGEX-2T vector was kindly provided by Prof. Junying Yuan at Harvard University. The protein sequence contains amino acid residues 1–212 of human Bcl- x_L plus a GST tag on the amino terminal. This protein was expressed in *E. coli* BL21 (DE3) cells. Cells were grown at 37 °C in LB medium containing 100 $\mu\text{g mL}^{-1}$ ampicillin to an OD_{600} value of 0.6. Protein expression was induced by 0.1 mM IPTG at 25 °C for 12 h. Cells were lysed in 50 mM Tris-HCl, pH 7.4 buffer containing 1 mM EDTA, 1% (v/v) Triton X-100, 5 mM DTT, 1x protease inhibitor cocktail, and 0.1 mg mL^{-1} PMSF. GST-tagged Bcl- x_L protein was purified via glutathione-affinity chromatography with GSTrapTM FF column (GE Healthcare) following the manufacturer's instructions.

Bcl-2: The Bcl-2 protein used in our study has the same construction as the one (Bcl-2/Bcl- x_L isoform 2) in the work of Fesik et al.,^[27] which is composed of amino acid residues 1–34 of human Bcl-2, amino acid residues 29–44 of human Bcl- x_L , and amino acid residues 92–207 of human Bcl-2. This construction has good solubility in water and reserves the biological function of human Bcl-2. It was cloned into the pGEX-4T1 vector at the EcoRI and XhoI sites, using the following oligonucleotides: 5'-TTT TGA ATT CAT GGC GCA CGC AGG TCG-3' and 5'-TTT TCT CGA GTC AAC GCA TGG ACG GGC-3'. Bcl-2 protein with an N-terminal GST tag was produced in *E. coli* BL21 (DE3) cells. Cells were grown at 37 °C in LB medium containing 100 $\mu\text{g mL}^{-1}$ ampicillin to an OD_{600} value of 0.6. Protein expression was induced by 0.2 mM IPTG at 25 °C for 12 h. Cells were lysed in 50 mM Tris-HCl, pH 7.4 buffer containing 1 mM EDTA, 1% (v/v) Triton X-100, 5 mM DTT, 1x protease inhibitor cocktail, and 0.1 mg mL^{-1} PMSF. GST-tagged Bcl-2 protein was purified via glutathione-affinity chromatography with GSTrapTM FF column (GE Healthcare) following the manufacturer's instructions.

Mcl-1: The Mcl-1 protein used in our study has the same construction as the one (hMcl-1^{BLR}) used in the work of Colman et al.,^[28] which is composed of amino acid residues 152–189 of mouse Mcl-1 and amino acid residues 209–327 of human Mcl-1. Such a construction has good solubility in water and reserves the biological function of human Mcl-1. It was cloned into the pSJ2 vector (a modified pET28a vector) at the HindIII and BamHI sites, using the following oligonucleotides: 5'-CCC CAA GCT TTT AAC CAC CTT CCA GGT CTT CAA C-3' and 5'-TTC CGG ATC CAT GGA AGA TGA TCT GTA CCG TCA GTC-3'. The Mcl-1 protein with an N-terminal 8xHis tag was expressed in *E. coli* BL21 (DE3) cells. Cells were grown at 37 °C in LB medium containing 100 $\mu\text{g mL}^{-1}$ ampicillin to an OD_{600} value of 0.6. Protein expression was induced by 0.4 mM IPTG at 37 °C for 4 h. Cells were lysed in 25 mM Tris-HCl, pH 8.0 buffer containing 300 mM NaCl, 5 mM β ME and 0.1 mg mL^{-1} PMSF. His-TEV-Mcl-1 protein was purified from the soluble fraction using Ni-NTA resin (QIAGEN), following the manufacturer's instructions. The His-TEV-Mcl-1 protein was further cleaved by TEV protease (0.5 mg mL^{-1} , 4 °C, 15 h) to produce the Mcl-1 protein.

In vitro binding assay

A fluorescence polarization (FP)-based assay was employed in our study to measure the binding of small-molecule compounds to all three Bcl-2 family proteins. Due to its technical convenience, the FP-based binding assay has been very popular for measuring the competitive binding of small-molecule compounds that disturb protein–protein interactions. In such a binding assay, a certain fluorescence-labeled polypeptide was used as the tracer. Competitive binding of a given compound was characterized quantitatively by monitoring the changes in FP signals after the addition of the compound under investigation at different concentrations.

Bcl- x_L : A 26-residue peptide derived from the BH3 domain on the Bim protein with 5-carboxy-fluorescein (5-FAM) on the N terminus, that is, 5-FAM-DMRPEIWIQAQELRRIGDEFNAYYARR, was used as the fluorescence tracer. Our experiments determined that this Bim-BH3 peptide binds to GST-Bcl- x_L with a K_d value of 43 nM (Figure 4a).

In our competitive binding experiments, Bcl- x_L and the test compound (in 1% [D_6]DMSO solution) were preincubated in the assay buffer (PBS, pH 7.3, 140 mM NaCl, 2.7 mM KCl, 10 mM Na_2HPO_4 , 1.8 mM KH_2PO_4) at 25 °C for 30 min. 20 μL of a FAM-Bim peptide solution in PBS was then added to this solution to produce a final volume of 200 μL and incubated at 25 °C for another 20 min. The total concentration of the Bim-BH3 peptide used in assay was 10 nM; whereas the total concentration of protein was 215 nM (five times the K_d value of the fluorescence tracer). Finally, the solutions were transferred into a Corning 384-well, black, flat-bottomed plates (60 μL per well, Corning Incorporated) and three wells were allocated per sample. The polarization values in milipolarization units (mP) were measured at an excitation wavelength of 485 nm and an emission wavelength of 535 nm using the Tecan GENios Pro Injector Reader (Tecan Group Ltd.). For each experiment, a control containing Bcl- x_L , Bim-BH3 peptide, and 1% (v/v) [D_6]DMSO (equivalent to 0% inhibition), and a second control containing only Bim-BH3, were included on each assay plate.

Bcl-2: A different fluorescence-labeled peptide was used in this case. This 26-residue peptide, (5-FAM-QEDIIRNIARHLAQVGDSMDR SIPP), was derived from the BH3 domain on the Bid protein. Our saturation experiments determined that this Bid-BH3 peptide binds to GST-Bcl-2 protein with a K_d value of 37 nM (Figure 4c). The experimental method for the competitive binding assay for GST-Bcl-2 was essentially the same as that for GST-Bcl- x_L except that the total concentration of GST-Bcl-2 was 185 nM (five times the K_d value of the fluorescence tracer).

Mcl-1: The same fluorescence-labeled Bid-BH3 peptide (5-FAM-QEDIIRNIARHLAQVGDSMDR SIPP) was used in this case. Our saturation experiments determined that this Bid-BH3 peptide binds to Mcl-1 protein with a K_d value of 60 nM (Figure 4e). The experimental settings of the competitive binding assay for Mcl-1 were essentially the same as those for GST-Bcl- x_L except that the total concentration of Mcl-1 was 300 nM (five times of the K_d value of the fluorescence tracer).

Both the 5-FAM-Bim-BH3 peptide and the 5-FAM-Bid-BH3 peptide used in our binding assay were ordered from the HD Biosciences Cooperation Company. The desired sequences were verified by amino acid component analysis and MS spectrum. Purity of these peptides was over 95% as verified by HPLC results. ABT-737 was used as a positive control in our binding assays. K_i values of ABT-737 measured in our assays against Bcl- x_L and Bcl-2 are 18 nM and 74 nM, respectively (Figure 4b and 4d). The reported IC_{50} values of

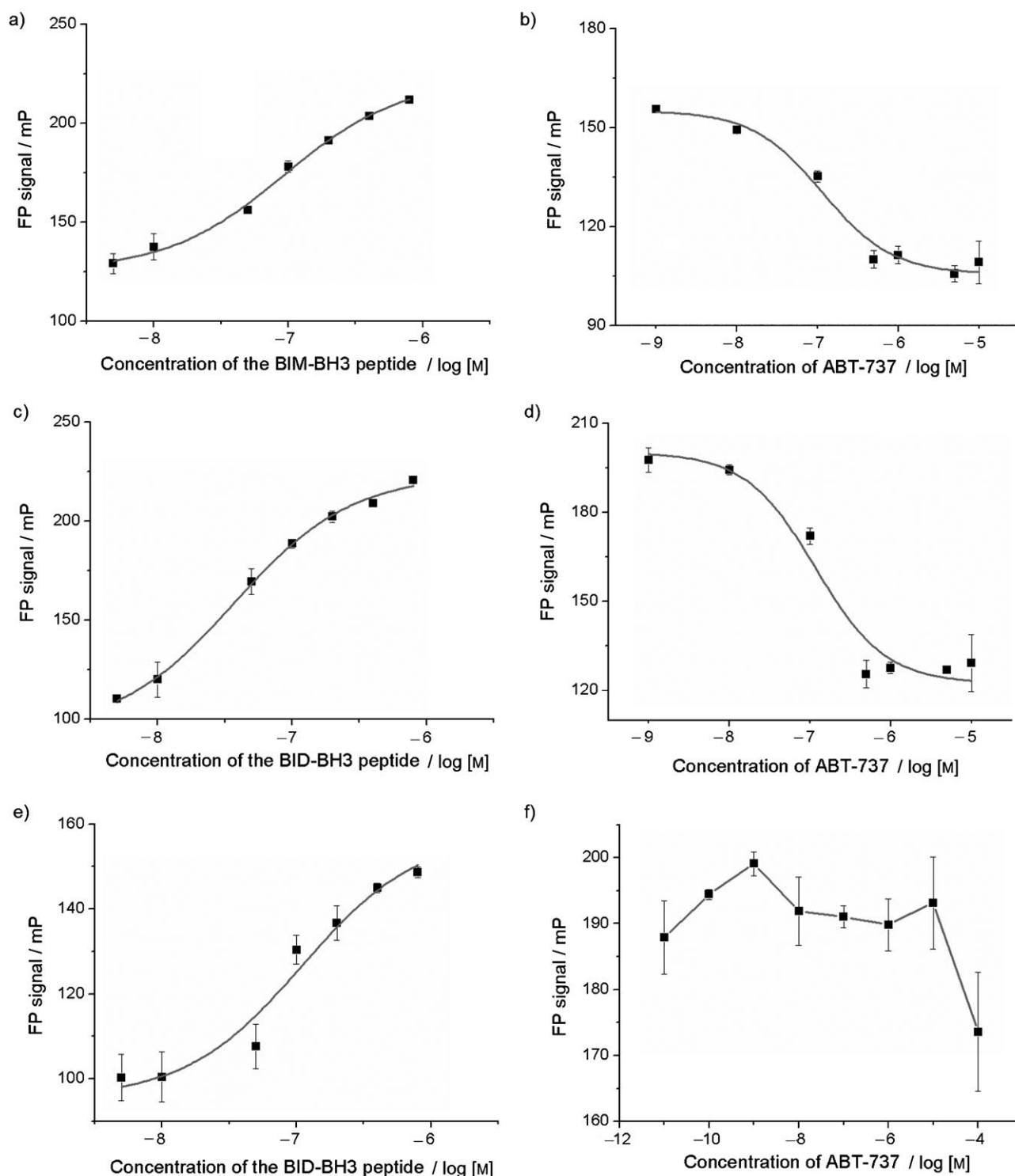


Figure 4. Dose-dependent results obtained in the FP assay for a) binding of the Bim-BH3 peptide to Bcl-x_L; b) competitive binding of ABT-737 to Bcl-x_L; c) binding of the Bid-BH3 peptide to Bcl-2; d) competitive binding of ABT-737 to Bcl-2; e) binding of the Bid-BH3 peptide to Mcl-1; f) competitive binding of ABT-737 to Mcl-1.

ABT-737 against Bcl-x_L and Bcl-2 are 35 nM and 103 nM (in the presence of 10% human serum), respectively.^[12,13] Thus, our results are consistent with the results reported in the literature. Our results also indicated that ABT-737 does not achieve a specific binding to Mcl-1 (Figure 4f). This observation is again consistent with what has been previously reported.^[12,13]

Each of our own compounds was tested against all three target proteins (Bcl-x_L, Bcl-2, and Mcl-1) at six different concentrations; 1 nM, 10 nM, 100 nM, 1 μM, 20 μM, and 50 μM. Once the dose-dependent binding curve was obtained, the concentration of the given compound at which 50% of the bound peptide was displaced (IC₅₀) was derived from the curve through non-linear fitting using the GraphPad Prism 5 software. The competitive inhibition

constant (K_i) of each tested compound was then calculated using Equation (1) developed by Wang et al.^[29] assuming that it forms a binary complex with the target protein.

$$K_i = [I]_{50} / ([L]_{50} / K_d + [P]_0 / K_d + 1) \quad (1)$$

In this equation, $[I]_{50}$ and $[L]_{50}$ denote the concentrations of the free small-molecule inhibitor (I) and the free fluorescence-labeled peptide ligand (L) at 50% inhibition, respectively, and $[P]_0$ is the concentration of the free protein (P) before the inhibitor is added, that is, 0% inhibition. To solve this equation, one needs to supply the total concentration of the protein used in the assay ($[P]_T$), the total concentration of the fluorescence-labeled ligand used in assay ($[L]_T$), the dissociation constant (K_d) between these two species, and the IC_{50} value of the tested compound as inputs. The first three parameters are constant for all tested compounds in our assay; whereas the last one can be derived from the corresponding dose-dependent inhibition curve of each tested compound. The computed K_i values of each tested compound on three target proteins are summarized in Table 1.

Heteronuclear single quantum coherence (HSQC) NMR

The Bcl-x_L protein used for this purpose was a special truncated construction of the full-length protein, with deletion of residues 45–84 on a large loop region and residues 210–233 at the C terminal. An 8×His tag was added to the N terminal. This protein was cloned into the pSJ2 vector (a modified vector based on pET28a) at the EcoRI and XhoI sites, using the following oligonucleotides: 5'-TCT CGA ATT CAT GTC TCA GAG CAA CCG GGA-3' and 5'-GGT CCT CGA GTC AGC GTT CCT GGC CCT TTC G-3'. It was expressed in *E. coli* BL21(DE3) cells. Cells were grown at 37 °C in M9 medium containing ¹⁵N-ammonium chloride and 1 mM ampicillin to an OD₆₀₀ value of 0.6. Protein expression was induced by 0.4 mM IPTG at 37 °C for 4 h. Cells were lysed in 25 mM Tris-HCl, pH 7.0 buffer containing 100 mM NaCl and 0.1 mg mL⁻¹ PMSF. ¹⁵N-labeled His-TEV-Bcl-x_L protein was purified from the soluble fraction using Ni-NTA resin (QIAGEN), following the manufacturer's instructions. The ¹⁵N-labeled His-TEV-Bcl-x_L protein was further cleaved by TEV protease (0.5 mg mL⁻¹, 4 °C, 12 h) to produce ¹⁵N-labeled Bcl-x_L protein. At last, the ¹⁵N-labeled Bcl-x_L protein was purified on a ResourceQ column (GE Healthcare) in the range from 100 mM to 1 M NaCl solution, Tris-HCl pH 7.5 and 5 mM DTT.

¹⁵N-Heteronuclear Single Quantum Correlation (HSQC) NMR spectra were recorded on a Bruker DMX 600 MHz NMR spectrometer at 25 °C with samples containing 200–500 μM of the ¹⁵N-labeled protein. The ratio of each tested compound and the Bcl-x_L protein in the sample was 1:1. The resulting NMR spectra were processed and analyzed using the NMRPipe and NMRDraw software. The HSQC spectrum of a complex structure formed between Bcl-x_L and Bad-BH3 peptide, which is publicly available from the Biological Magnetic Resonance Data Bank (<http://www.bmrb.wisc.edu/>, access number=6578), was adopted as the reference for assignment of chemical shifts.

The Bim-BH3 peptide (DMRPEIWIQAQLRRIGDEFNAYYARR, a 26-mer) and ABT-737 are known to bind to the BH3 binding groove on Bcl-x_L. These two compounds were thus used as positive controls in our HSQC NMR measurements. To identify the amino acid residues on Bcl-x_L affected by the binding of BCL-LZH-02, we compared the HSQC spectra of Bcl-x_L with the presence of BCL-LZH-02 to those of Bcl-x_L with the Bim-BH3 peptide and ABT-737. The amino acid residues on Bcl-x_L affected by the binding of BCL-LZH-

02 overlapped closely with those involved in the binding of the Bim-BH3 peptide and ABT-737. This observation indicates that BCL-LZH-02 binds to the same binding site on Bcl-x_L as the Bim-BH3 peptide and ABT-737.

Molecular modeling

Molecular docking was employed to predict the binding modes of selected molecules to the Bcl-x_L protein. The three-dimensional structure of Bcl-x_L was taken from Protein Data Bank (PDB entry 1BXL), a NMR-resolved structure of Bcl-x_L in complex with the Bak-BH3 peptide. Note that the Bcl-x_L protein has a somewhat flexible binding pocket. This particular Bcl-x_L structure was chosen in our modeling study as its binding site has a suitable size for accommodating most of our compounds. In addition, this structure does not have any missing segment so that no extra efforts are needed before it can be used in molecular modeling studies.

Automatic docking of each ligand molecule to Bcl-x_L was performed by using the GOLD software (version 5.0, released by the CCDC Inc). The binding site considered in docking was defined as all amino acid residues within 18 Å from Gly138, which is located roughly at the center of the binding site on Bcl-x_L. In each case, a rough binding pose was provided as the starting point. As our ¹⁵N-HSQC results indicated that our compounds bound at the same site on Bcl-x_L as ABT-737, the rough binding pose of each compound was derived manually by overlapping its minimized structure onto the known binding pose of ABT-737. GOLD essentially employs a genetic algorithm (GA) to control the docking process. In our study, the whole population was placed on five separate islands with 100 individuals on each island. The total number of GA operations to be performed was set to 300 000. Probabilities for crossover, mutation, and migration operations were set to 95, 95, and 10 respectively. The ChemScore scoring function was adopted to compute the fitness scores of each binding pose. A total of 30 final binding poses were generated for each input molecule. These binding poses were clustered with a RMSD cutoff of 2.0 Å using the "rms analysis" tool included in the GOLD software package. Among the binding poses with the highest binding scores in each cluster, one was selected after visual examination as the most reasonable one for further consideration.

Binding poses of all of the compounds, except for five compounds inactive in the binding assay (Table 1), were derived through the molecular docking procedure described above. Their binding scores were computed with the ChemScore scoring function implemented in the GOLD software. The correlation between the calculated binding scores and experimentally measured binding data ($-\log K_i$) of our compounds is fairly good (Figure 5), indicating that the binding modes of the compounds derived in our study are reasonable.

Note that there is a chiral center on the dihydropyrimidine ring in the chemical structure of this class of compounds, and the absolute configuration of this chiral center has not been resolved so far. To provide a more rational basis for analyzing the structure–activity relationship of this class of compounds, we actually derived the binding modes of both the *R* and *S* enantiomer of the template compound (BCL-LZH-02) through the molecular docking procedure described above. The binding modes of the two enantiomers were further evaluated by molecular dynamics (MD) simulations. All MD simulations in our study were performed by using the AMBER program (version 9). The force field parameters applied to the small-molecule ligand were prepared by applying the Antechamber module in AMBER. Atomic partial charges on the small-molecule

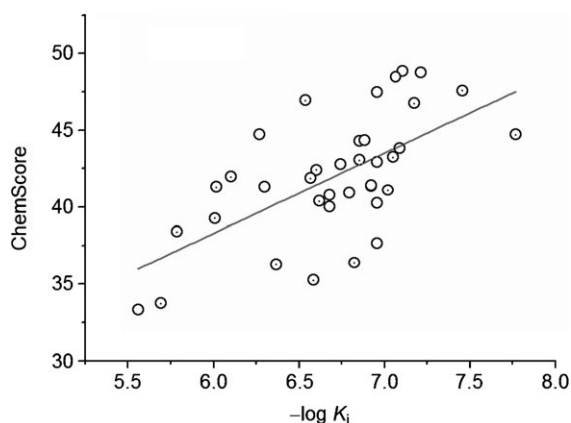


Figure 5. Correlation between calculated binding scores and experimentally measured binding data ($-\log K_i$) of our compounds: $n = 38$, $r = 0.63$, $SD = 0.52 \text{ kcal mol}^{-1}$.

ligand were derived with the RESP method based on the HF/6-31G* computation results given by the Gaussian software (version 09, released by the Gaussian Inc). Atoms on the Bcl-x_L protein were assigned according to the PARM99 template charges implemented in AMBER, and all ionizable residues were set at the default protonation states at a neutral pH. The complex structure was soaked in a box of TIP3P water molecules with a margin of 10 Å along each dimension. An appropriate number of counter ions were added to neutralize the whole system. The complex structure was subjected to energy minimization to release internal repulsions. After that, the whole system was gradually heated with the Berendsen algorithm from 0 K to 300 K in 100 ps. Then, a MD simulation of 3 ns was performed for each complex at a constant temperature of 300 K and a constant pressure of 1 atm. The time interval was set to 2 fs. In all MD simulations performed in our study, the SHAKE method was employed for constraining all covalent bonds connecting hydrogen atoms, but no other constraints were applied. The General AMBER Force Field (GAFF) was employed to compute internal energies with a nonbonded distance cutoff of 12 Å. The Particle Mesh Ewald (PME) method was employed for handling long-range electrostatic interactions. The last snapshot on the resulting MD trajectory was retrieved and subjected to further energy minimization to obtain the final binding mode of the ligand molecule under study.

Based on the outcomes of MD simulations, the MM-GB/SA method implemented in the AMBER software was used to compute the binding free energies between each ligand molecule and the Bcl-x_L protein. The results indicated that (R)-BCL-LZH-02 bound to Bcl-x_L more tightly than (S)-BCL-LZH-02 (−14.7 kcal/mol versus −9.3 kcal/mol). Accordingly, the binding modes shown in Figure 2 and Figure 3 are those of (R)-BCL-LZH-02 and (R)-BCL-LZH-40, respectively. More details on the MD simulations and MM-GB/SA computations performed in our study can be found in the Supporting Information.

Supporting Information

More detailed descriptions concerning the methods and results of the molecular modeling study of our compounds are available by contacting the corresponding author.

Acknowledgements

The authors are grateful to the financial supports from the Chinese National Natural Science Foundation (grants no.: 90813006, 21072213, 21002117, and 20921091), the Chinese Ministry of Science and Technology (grant no.: 2009ZX09501-002), and the Science and Technology Commission of Shanghai Municipality (P. R. China) (grant no.: 074319113). The authors also thank Prof. Junying Yuan (Harvard University, USA) and Prof. Shaomeng Wang (University of Michigan, USA) for providing some experimental material and helpful advice.

Keywords: Bcl-2 family proteins • inhibitors • protein–protein interactions • small molecules • structure-based drug design

- [1] D. R. Green, J. C. Reed, *Science* **1998**, *281*, 1309–1312.
- [2] G. Evan, T. Littlewood, *Science* **1998**, *281*, 1317–1322.
- [3] S. Cory, J. M. Adams, *Nat. Rev. Cancer* **2002**, *2*, 647–656.
- [4] J. C. Reed, *Nat. Rev. Drug Discovery* **2002**, *1*, 111–121.
- [5] S. W. Fesik, *Nat. Rev. Cancer* **2005**, *5*, 876–885.
- [6] M. H. Andersen, J. C. Becker, P. Straten, *Nat. Rev. Drug Discovery* **2005**, *4*, 399–409.
- [7] S. Pattingre, A. Tassa, X. P. Qu, R. Garuti, X. H. Liang, N. Mizushima, M. Packer, M. D. Schneider, B. Levine, *Cell* **2005**, *122*, 927–939.
- [8] Y. M. Janumyan, C. G. Sansam, A. Chattopadhyay, N. L. Cheng, E. L. Soucie, L. Z. Penn, D. Andrews, C. M. Knudson, E. Yang, *EMBO J.* **2003**, *22*, 5459–5470.
- [9] M. Arkin, *Curr. Opin. Chem. Biol.* **2005**, *9*, 317–324.
- [10] A. G. Letai, *Nat. Rev. Cancer* **2008**, *8*, 121–132.
- [11] G. Lessene, P. E. Czabotar, P. M. Colman, *Nat. Rev. Drug Discovery* **2008**, *7*, 989–1000.
- [12] T. Oltersdorf, S. W. Elmore, A. R. Shoemaker, R. C. Armstrong, D. J. Augeri, B. A. Belli, M. Bruncko, T. L. Deckwerth, J. Dinges, P. J. Hajduk, M. K. Joseph, S. Kitada, S. J. Korsmeyer, A. R. Kunzer, A. Letai, C. Li, M. J. Mitten, D. G. Nettesheim, S. Ng, P. M. Nimmer, J. M. O'Connor, A. Oleksiewicz, A. M. Petros, J. C. Reed, W. Shen, S. K. Tahir, C. B. Thompson, K. J. Tomaselli, B. Wang, M. D. Wendt, H. Zhang, S. W. Fesik, S. H. Rosenberg, *Nature* **2005**, *435*, 677–681.
- [13] C. Tse, A. R. Shoemaker, J. Adickes, M. G. Anderson, J. Chen, S. Jin, E. F. Johnson, K. C. Marsh, M. J. Mitten, P. Nimmer, L. Roberts, S. K. Tahir, Y. Xiao, X. Yang, H. Zhang, S. Fesik, S. H. Rosenberg, S. W. Elmore, *Cancer Res.* **2008**, *68*, 3421–3428.
- [14] A. Degterev, A. Lugovskoy, M. Cardone, B. Mulley, G. Wagner, T. Mitchinson, J. Yuan, *Nat. Cell Biol.* **2001**, *3*, 173–182.
- [15] S. Kitada, M. Leone, S. Sareth, D. Zhai, J. C. Reed, M. Pellecchia, *J. Med. Chem.* **2003**, *46*, 4259–4264.
- [16] B. Becattini, S. Kitada, M. Leone, E. Monosov, S. Chandler, D. Zhai, T. J. Kipps, J. C. Reed, M. Pellecchia, *Chem. Biol.* **2004**, *11*, 389–395.
- [17] M. Nguyen, R. C. Marcellus, A. Roulston, M. Watson, L. Serfass, S. R. Murthy Madiraju, D. Goulet, J. Viallet, L. Belec, X. Billot, S. Acoca, E. Purisima, A. Wiegman, L. Cluse, R. W. Johnstone, P. Beauparlant, G. C. Shore, *Proc. Natl. Acad. Sci. USA* **2007**, *104*, 19512–19517.
- [18] G. Wang, Z. Nikolovska-Coleska, C. Y. Yang, R. Wang, G. Tang, J. Guo, S. Shangary, S. Qiu, W. Gao, D. Yang, J. Meagher, J. Stuckey, K. Krajewski, S. Jiang, P. P. Roller, H. O. Abaan, Y. Tomita, S. Wang, *J. Med. Chem.* **2006**, *49*, 6139–6142.
- [19] G. Tang, Z. Nikolovska-Coleska, S. Qiu, C. Y. Yang, J. Guo, S. Wang, *J. Med. Chem.* **2008**, *51*, 717–720.
- [20] J. Wei, J. L. Stebbins, S. Kitada, R. Dash, W. Placzek, M. F. Rega, B. Wu, J. Cellitti, D. Zhai, L. Yang, R. Dahl, P. B. Fisher, J. C. Reed, M. Pellecchia, *J. Med. Chem.* **2010**, *53*, 4166–4176.
- [21] Y. Futamura, R. Sawa, Y. Umezawa, M. Igarashi, H. Nakamura, K. Hasegawa, M. Yamasaki, E. Tashiro, Y. Takahashi, Y. Akamatsu, M. Imoto, *J. Am. Chem. Soc.* **2008**, *130*, 1822–1823.
- [22] S. Kolb, O. Mondesert, M. L. Goddard, D. Jullien, B. O. Villoutreix, B. Ducommun, C. Garbay, E. Braud, *ChemMedChem* **2009**, *4*, 633–648.

- [23] M. Sattler, H. Liang, D. Nettesheim, R. P. Meadows, J. E. Harlan, M. Eberstadt, H. S. Yoon, S. B. Shuker, B. S. Chang, A. J. Minn, C. B. Thompson, S. W. Fesik, *Science* **1997**, 275, 983–986.
- [24] P. Biginelli, *Gazz. Chim. Ital.* **1893**, 23, 360–413.
- [25] T. S. Jin, S. L. Zhang, T. S. Li, *Synth. Commun.* **2002**, 32, 1847–1851.
- [26] B. Sridhar, K. Ravikumar, Y. S. Sadanandam, *Acta Crystallogr., Sect. C: Cryst. Struct. Commun.* **2006**, 62, o687–o690.
- [27] A. M. Petros, A. Medek, D. G. Nettesheim, D. H. Kim, H. S. Yoon, K. Swift, E. D. Matayoshi, T. Oltersdorf, S. W. Fesik, *Proc. Natl. Acad. Sci. USA* **2001**, 98, 3012–3017.
- [28] P. E. Czabotar, E. F. Lee, M. F. van Delft, C. L. Day, B. J. Smith, D. C. Huang, W. D. Fairlie, M. G. Hinds, P. M. Colman, *Proc. Natl. Acad. Sci. USA* **2007**, 104, 6217–6222.
- [29] Z. Nikolovska-Coleska, R. Wang, X. Fang, H. Pan, Y. Tomita, P. Li, P. P. Roller, K. Krajewski, N. G. Saito, J. A. Stuckey, S. Wang, *Anal. Biochem.* **2004**, 332, 261–273.

Received: December 11, 2010

Published online on February 25, 2011